

**STUDIES ON PHOTO STABILIZATION OF PYRETHRUM  
FLOWER EXTRACTS USING CLAY**

**ESTHER WAMAITHA MAINA**

**MASTER OF SCIENCE  
(Chemistry)**

**JOMO KENYATTA UNIVERSITY OF  
AGRICULTURE AND TECHNOLOGY**

**2016**

**Studies on Photo Stabilization of Pyrethrum Flower Extracts using  
Clay**

**Esther Wamaitha Maina**

**A Thesis Submitted in Partial Fulfillment of the Requirements for the  
Award of the Degree of Master of Science in Chemistry in the School of  
Physical Sciences in Jomo Kenyatta university of Agriculture and  
Technology**

**2016**

## DECLARATION

This thesis is my original work and has not been presented for a degree in any other university.

Signature..... Date.....

**Maina Esther Wamaitha**

This thesis has been submitted for examination with our approval as university supervisors.

Signature..... Date.....

**Dr. Harrison N. Wanyika**

**JKUAT, Kenya**

Signature..... Date.....

**Prof. Anthony Gachanja**

**JKUAT, Kenya.**

## **DEDICATION**

This work is dedicated to my family. Special dedication to my dad, Gidraph Maina, mum, Priscillah Maina, sister, Carol Maina and to my husband and a great friend Paul Waweru for their love and spiritual advice to my life.

## **ACKNOWLEDGEMENTS**

First, I thank Almighty God for His many blessings He has granted me. I would also like to express my deep thanks and great appreciation to my supervisors; Dr. Harrison Wanyika and Prof. Anthony Gachanja for their advice, continuous help, support and encouragement throughout the research period.

I would also like to thank NACOSTI for funding the research and the Department of Chemistry, JKUAT for their support in form of facilities and laboratory space.

I would never be able to thank enough my family for the unconditional love and support that they have always shown me. I owe them my most sincere and deep gratitude.

Lastly, and not the least my gratitude goes to my fellow graduate students who worked with me on the bench for all the support, care and positive criticism.

## TABLE OF CONTENTS

<b>DECLARATION</b> .....	ii
<b>DEDICATION</b> .....	iii
<b>ACKNOWLEDGEMENTS</b> .....	iv
<b>TABLE OF CONTENTS</b> .....	v
<b>LIST OF FIGURES</b> .....	ix
<b>LIST OF SYMBOLS</b> .....	xi
<b>LIST OF APPENDICES</b> .....	xii
<b>ABSTRACT</b> .....	xiv
<b>CHAPTER ONE</b> .....	91
<b>1.0 INTRODUCTION AND LITERATUE REVIEW</b> .....	91
1.1 Background of the study.....	91
1.2 Pyrethrum flower.....	93
1.3 Clay materials.....	94
1.4 Organo clays synthesis and their applications.....	95
1.5 Cation exchange capacity .....	96
1.6 Characterization of clays .....	97
1.6.1 Fourier transform infrared (FT-IR) Spectroscopy .....	97
1.6.2 X-ray diffractometry .....	98
1.6.3 X-Ray Florescence.....	99
1.7 Adsorption isotherms .....	99
1.7.1 Kinetic models of sorption.....	100
1.8 Storage of cereals .....	100
1.9 Botanical control of Cereals .....	101
1.10 Statement of the problem .....	102
1.11 Justification .....	102
1.12 Hypothesis .....	103

1.13 Objectives .....	103
1.13.1 General Objective .....	103
1.13.2 Specific objectives .....	103
<b>CHAPTER TWO</b> .....	<b>105</b>
<b>2.0 MATERIALS AND METHODS</b> .....	<b>105</b>
2.1 Research designs .....	105
2.2 Solvents and reagents .....	105
2.3 Preparation of standards .....	105
2.4 Collection of clay samples and pretreatment .....	105
2.5 Isolation of clays .....	107
2.6 Characterization of the clays .....	107
2.6.1 Elemental analysis using total x-ray fluorescence spectrometry (TXRF) .....	107
2.6.2 Determination of basal spacing and crystallite size.....	108
2.6.3 Determination of cation exchange capacity (CEC) of clay .....	109
2.6.4 Functional groups determination using fourier transform-infrared (FT-IR) spectroscopy.....	110
2.6.5 UV-Visible spectrophotometry for determination of transitional groups.....	110
2.7 Preparation of organo clay .....	111
2.8 Determination of sorption kinetics of PFE into clay materials .....	112
2.8.1 Determination of pH .....	112
2.8.2 Effect of temperature .....	113
2.8.3 Determination of initial concentration and contact time .....	113
2.8.4 Effect of sorbent dosage .....	113
2.9 Loading of PFE into clay materials.....	114
2.10 Accelerated photo stability test .....	114
2.11 Bioassay tests on maize weevils using clay samples .....	115
2.11.1 <i>Sitophilus zeamais</i> motschulsky culture.....	115
2.11.2 Bioassay .....	115
<b>CHAPTER THREE</b> .....	<b>117</b>

<b>3.0 RESULTS AND DISCUSSION</b> .....	117
3.1 Purification of clays.....	117
3.2 Characterization of the clays .....	118
3.2.1 TXRF Elemental composition .....	118
3.2.2 The FT-IR spectra of the clays .....	119
3.2.3 UV-Visible spectra .....	121
3.2.4 The XRD Analysis.....	122
3.2.5 CEC of the clays .....	125
3.3 HDTMA and TMPA modified clays.....	127
3.3.1 FT-IR spectra .....	127
3.3.2 XRD Analysis.....	128
3.4 PFE sorption kinetics.....	130
3.4.1 The effect of pH.....	130
3.4.2 Effect of temperature .....	131
3.4.3 Effect of initial concentration and contact time.....	132
3.4.4 Effect of adsorbent dose .....	133
3.4.5 Sorption isotherms .....	134
3.4.6 Kinetic sorption models .....	136
3.5 Intercalation of PFE in clay materials .....	140
3.6 Accelerated stability test .....	142
3.6.1 Photo-degradation of pyrethrins .....	144
3.6.1.1 The photo-chemical reaction.....	144
3.6.1.2 Photo-protection of the clays and organo clays to PFE pesticides.....	145
3.7 Bioassay tests on maize weevils.....	146
<b>CHAPTER FOUR</b> .....	150
<b>4.0 CONCLUSION AND RECOMMENDATIONS</b> .....	150
4.1 CONCLUSIONS .....	150
4.2 RECOMMENDATIONS .....	151
4.2.1 Recommendations from this work.....	151

4.2.2 Recommendations for further work ..... 151

### LIST OF TABLES

**Table 1.1:** Some selected organic cations..... 95

**Table 3.1:** Oxide levels (%) of the clay samples ..... 118

**Table 3.2:** The FT-IR absorption bands of different clay samples..... 121

**Table 3.3:** Total CEC of the different clays ..... 127

**Table 3.4:** Basal spacing increment on organic cations intercalation in clay..... 130

**Table 3.5:** Langmuir and Freundlich parameters ..... 135

**Table 3.6:** Pseudo-first and pseudo-second order reaction kinetics for the sorption of PFE on the un-modified, TMPA modified and HDTMA modified clays.... 137

**Table 3.7:** Basal spacing variations on PFE intercalation in clay gallery spaces..... 141

**Table 3.8:** Analysis of Variance (ANOVA) for the different carriers at different dosage rates ..... 147

**Table 3.9:** Cumulative means of different clay treatments on maize weevils (*Sitophilus zeamais*) mortality rate..... 148

## LIST OF FIGURES

<b>Figure 1.1:</b>	Pyrethrins esters; (a) pyrethrin I, (b) pyrethrins II, (c) cinerin I, (d) cinerin II, (e) jasmolin I and (f) jasmolin II .....	<b>92</b>
<b>Figure 1.2:</b>	Structure of montmorillonite clay .....	<b>94</b>
<b>Figure 1.3:</b>	Schematic diagram illustrating XRD diffraction .....	<b>98</b>
<b>Figure 2.1:</b>	Sample collection area .....	<b>106</b>
<b>Figure 3.1:</b>	Different clay sample purification methods .....	<b>117</b>
<b>Figure 3.2:</b>	Elemental composition (ppm) of different clay samples .....	<b>118</b>
<b>Figure 3.3:</b>	FT-IR spectra of clay samples; (a) A, (b) B, (c) C and (d) D .....	<b>119</b>
<b>Figure 3.4:</b>	UV-Visible Spectra of: (a) clay A, (b) clay B, (c) clay C and (d) clay D ....	<b>122</b>
<b>Figure 3.5:</b>	X-ray diffraction patterns of unmodified clay minerals at different sample treatment; (a) treated with Ethylene Glycol and (b) heated at high temperatures of 550 °C .....	<b>123</b>
<b>Figure 3.6:</b>	A concentration versus absorbance curve for; (a) $Mg^{2+}$ (b) $Ca^{2+}$ and (c) $Na^+$ and $K^+$ .....	<b>126</b>
<b>Figure 3.7:</b>	FT-IR spectra for clay (a) modified with TMPA and (b) modified with HDTMA .....	<b>127</b>
<b>Figure 3.8:</b>	XRD diffraction patterns for different clay materials .....	<b>129</b>
<b>Figure 3.9:</b>	The effect of pH on the sorption of PFE into different clay materials; (a) unmodified (b) TMPA modified and (c) HDTMA modified clay materials....	<b>131</b>
<b>Figure 3.10:</b>	Effect of temperature on sorption of PFE into different clay materials; (a) un-modified Clay, (b) TMPA modified clay and (c) HDTMA modified clay	<b>132</b>
<b>Figure 3.11:</b>	Effect of initial concentrations at different contact time on the sorption of PFE into; (a) un-modified clay, (b) TMPA modified clay and (c) HDTMA modified clay .....	<b>133</b>
<b>Figure 3.12:</b>	Sorption of PFE in relation to different clay adsorbate dose; (a) Un-Modified Clay, (b) TMPA Modified Clay and (c) HDTMA Modified Clay .....	<b>134</b>

<b>Figure 3.13:</b>	Langmuir (a) and Freundlich (b) adsorption isotherms plots.....	<b>135</b>
<b>Figure 3.14:</b>	Pseudo first order kinetics model for the sorption of PFE into (a) un-modified clay, (b) TMPA modified clay and (c) HDTMA modified clay ...	<b>138</b>
<b>Figure 3.15:</b>	second order kinetics model for the sorption of PFE into; (a) un-modified clay, (b) TMPA modified clay and (c) HDTMA modified clay at different concentrations.....	<b>139</b>
<b>Figure 3.16:</b>	FT-IR spectra of; (a) PFE intercalated in un-modified clay; (b) PFE in TMPA modified clay and (c) PFE in HDTMA modified clay.....	<b>140</b>
<b>Figure 3.17:</b>	The XRD patterns of PFE intercalated in different clay materials .....	<b>141</b>
<b>Figure 3.18:</b>	(a) A HPLC chromatogram for (a) concentration versus peak area calibration curve for PFE together with (b) pyrethrins standard, (c) pyrethrins at HDTMA modified clay after 4 hours natural sunlight exposure and (d) control PFE after 4 hours natural sunlight .....	<b>142</b>
<b>Figure 3.19:</b>	Protective effect of different clay materials on PFE pesticide; (a) PFE in clay and (b) control PFE .....	<b>143</b>
<b>Figure 3.20:</b>	Degradation of pyrethrins by UV light .....	<b>145</b>
<b>Figure 3.21:</b>	Mortality rate (%) of maize weevils ( <i>Sitophilus zeamais</i> ) at different dosage rates within different carriers administered at varying times.....	<b>148</b>

## LIST OF SYMBOLS

$K_f$	Freundlich constant
$Q_e$	Total sorption at equilibrium
$Q^0$	Langmuir constant
$Q_t$	Total sorption at equilibrium
$R^2$	Correlation coefficient
$\bar{X}$	Mean

## LIST OF APPENDICES

<b>Appendix 1:</b>	Mean ( $\bar{x} \pm SD$ ) elemental composition (ppm) of different clay samples	<b>163</b>
<b>Appendix 2:</b>	Crystallite claysize .....	<b>164</b>
<b>Appendix 3:</b>	The CEC of magnesium ions in clay samples.....	<b>164</b>
<b>Appendix 4:</b>	The CEC of calcium ions in clay samples .....	<b>164</b>
<b>Appendix 5:</b>	The CEC of sodium ions in clay samples .....	<b>165</b>
<b>Appendix 6:</b>	The CEC of potassium ions in clay samples.....	<b>165</b>
<b>Appendix 7:</b>	Sorption capacity of PFE at different pH in various clay samples .....	<b>165</b>
<b>Appendix 8:</b>	Sorption capacity of PFE at different adsorbate dose in various clay samples.....	<b>166</b>
<b>Appendix 9:</b>	Langmuir concentration at equilibrium versus sorption capacity of various clay materials.....	<b>166</b>
<b>Appendix 10:</b>	Freundlich concentration at equilibrium versus sorption capacity in different clay materials.....	<b>167</b>
<b>Appendix 11:</b>	Pseudo first order values for sorption of PFE in various clay materials	<b>168</b>
<b>Appendix 12:</b>	Pseudo second order values for sorption of PFE in various clay materials .....	<b>169</b>
<b>Appendix 13:</b>	Percentage PFE degraded both in different clay materials and in unprotected (control) PFE.....	<b>170</b>
<b>Appendix 14:</b>	Effect of different treatments on <i>Sitophilus zeamais</i> mortality rate ....	<b>171</b>
<b>Appendix 15:</b>	FT-IR Spectra of (a) HDTMA and (b) TMPA organic cations .....	<b>171</b>

## **LIST OF ABBREVIATIONS AND ACRONYMS**

<b>CEC</b>	Cation Exchange Capacity
<b>HDTMA</b>	Hexadecyltrimethyl ammonium
<b>HPLC</b>	High Performance Liquid Chromatography
<b>MMT</b>	Montmorillonite
<b>PBK</b>	Pyrethrum Board of Kenya
<b>PFE/ NPE</b>	Pyrethrum Flower Extracts / Natural Pyrethrum Extracts
<b>Rpm</b>	Rotations per minute
<b>TPMA</b>	Trimethyl phenyl ammonium bromide
<b>TXRF</b>	Total Reflection X-ray Florescence
<b>UV</b>	Ultraviolet
<b>XRD</b>	X-ray Diffraction

## ABSTRACT

The use of botanical pesticide in the agricultural sector over synthetic pesticide would ensure less pest resistance and reduced environmental pollution. Pyrethrins are effective, environmental friendly pesticides, but are photo-labile, limiting their use in pest control. Clay is a natural occurring mineral and its photo-stabilization of pyrethrins would result in formulation of environmental friendly pesticide. In the present study, montmorillonite (MMT) clays were obtained from natural clay by sedimentation and centrifugation techniques. Organo-clays were prepared by treating the clay with Hexadecyltrimethylammonium bromide (HDTMA) and Trimethylphenylammonium Bromide (TMPA) organic cations. Pyrethrins molecules were loaded onto these organo-clays by mixing them with the pyrethrins solutions to obtain pyrethrins-organo clay composites and the samples were characterized using Fourier Transform Infrared (FT-IR) spectroscopy and X-ray Diffractometry (XRD) techniques. *In vitro* photo stability tests were done using artificial UV light at 254 nm and 366 nm and *in situ* tests by exposing the Pyrethrins-clay composite products in sunlight for four hours. Different sample treatments exposed to UV light were used against maize weevils to test their efficacy. The findings demonstrated that HDTMA cations were intercalated more in the MMT clay materials in comparison to TMPA cation. This consequently resulted to more sorption of PFE's molecules sorption into the HDTMA-clay composites. A great potential of clay to photo stabilize PFE and consequently improve the efficacy of PFE-based pesticides. Bioassay test on maize weevils revealed 100 % mortality rate on PFE HDTMA-clay treatments at 120 hours while the un-protected PFEs exhibited 18% mortality rate for the same duration of time. Pyrethrins were highly photo-stabilized by HDTMA-clay reducing in its photo-degradation. Bioassay study showed that PFE-HDTMA clay can be a potential maize grain protectant against maize weevils (*Sitophilus zeamais*) due to considerable mortality rates at low dosage. Successful photo-stabilization of the pyrethrins pesticide based formulation would improve the

marketability of the pyrethrum flowers, improve economic utilization of clay deposits and consequently boost food security in Kenya and globally at large

# CHAPTER ONE

## INTRODUCTION AND LITERATURE REVIEW

### 1.1 Background of the study

Synthetic pesticides use for agricultural purposes have resulted in environmental pollution due to low degradation rate in the environment. The processes through which they get into the environment are through pesticide degradation by photolysis, run offs and volatization (Wanyika, 2014; Yakan *et al.*, 2015). There is thus a growing demand for a low health risk, conservation of ecosystems and a biological diversity product (Blankson *et al.*, 2014; Isman, 2008; Sola *et al.*, 2014). Mann *et al.*, (2012), discussed the importance of use of natural chemicals as they are safer than conventional pesticide due to rapid degradation and environmental friendly nature.

Among the botanicals products being traded globally are the pyrethrum products from *Chrysanthemum cinerariaefolium*, Neem products from *Azadirachta indica*Juss and rotenone from *Derrismalaccensis*. Pyrethrum extracts are a combination of six natural esters of chrysanthemic acid; pyrethrins I and II, Jasmolin I and II and Cinerin I and II (Figure1.1) extracted from pyrethrum flowers (*Chrysanthemum cinerariaefolium*)which are the active groups.

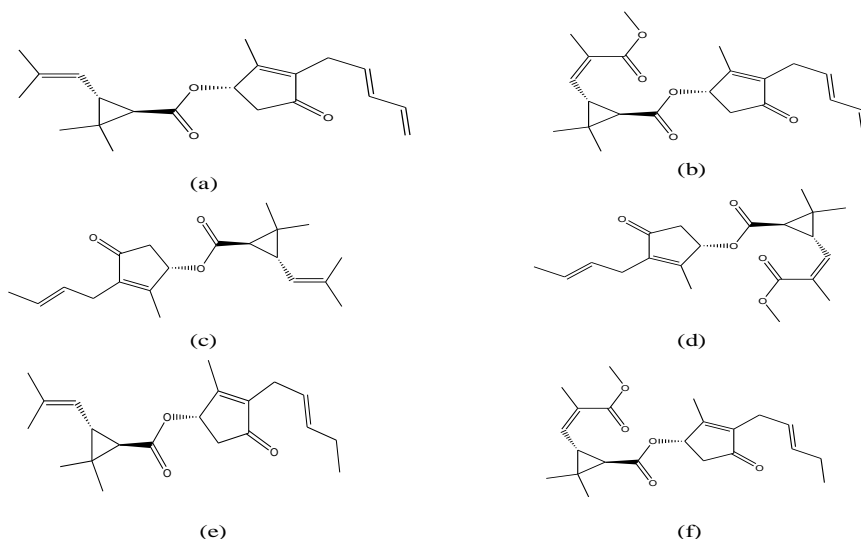


**Figure 1.1: Pyrethrins esters; (a) pyrethrin I, (b) pyrethrins II, (c) cinerin I, (d) cinerin II, (e) jasmolin I and (f) jasmolin II**

Pyrethrin I, cinerin I and jasmolin I are esters of chrysanthemic acid which differ from each other in the side chains attached to the cyclopentanolone ring. Pyrethrins II, cinerin II and jasmolin II are also related and they are esters of pyrethric acid (Wanyika *et al.*, 2009). These compounds are responsible for the quick knockdown properties of the pesticide and are safer to use (Sola *et al.*, 2014). The extracts are commonly used to formulate an end-use pesticide product (Essig & Zhau, 2001).

According to Housset and Dickmann, (2009), the benefits associated with pyrethrum extracts pesticide development is difficult to estimate as it can be assessed in many different ways. Thousands of the houses have been protected against termites, tens of thousands of restaurants, hospitals, ships and airplanes have been saved from pest attacks. Millions of people saved from diseases such as malaria, allergies, and thus placing it in the lead in terms of achievements.

Photo degradation of the pyrethrins is rapid in presence of UV light (Atkinson *et al.*, (2004). Pyrethrins formulations based on lignin-derivatives provided extended simulated sunlight protection (Fernandez-Perez *et al.*, 2014). Plant extracts can also act as photo-

stabilizing agents of the active ingredients (Eyheraguibel *et al.*, 2010). Wanyika *et al.*, (2009), observed that the natural pyrethrum extracts can be photo stabilized using fixed plant oils and tea extracts. The results indicated that the efficacy against the insect eradication (maize weevils), increased when cotton seed oil was used due to it having the highest photo stabilizing effect on the pyrethrum natural extracts.

## **1.2 Pyrethrum flower**

Kenya initially was the world's largest producer of natural pyrethrum where it has been grown as a crop for over 70 years and is currently being grown in Tanzania, Uganda and Rwanda (Sola *et al.*, 2014). In 1993/ 1994 the country's production was at the peak to about 88% of the world's produce (Sola *et al.*, 2014). Production has since declined due to poor supply chain management. However, according to the Government of Kenya (2013), the industry is expected to pick up after replacement of Pyrethrum Board of Kenya (PBK) with Pyrethrum Regulatory Authority body where investors and private sectors have been allowed into the industry.

Pyrethrum refers to plant flower head or flower extract with the active insecticidal components of pyrethrum being pyrethrins (Morris *et al.*, 2006). Pyrethrins affect the nervous system of the insects, blocking the nerve junctions and the action of sodium channels. Pyrethrins have advantages in that they are effective at low dosage, controls wide range of pests, less toxicity to mammals, rapid degradation on exposure to UV light and lack of accumulation in food chains and ground water. Formulation of these pyrethrins with antioxidants, stabilizers and synergists will improve on the instability (Jana, 2007).

### 1.3 Clay materials

Clay materials are abundant in most continents of the world and are familiar due to their low cost, high sorption properties, ion exchange and good adsorbent properties (Gupta *et al.*, 2013). These clay materials are characterized by their layered structures which results to different classes of clays such as smectites (montmorillonite), Mica (illite), kaolinite, serpentine, vermiculite and sepiolite. Montmorillonite (MMT) clay (Figure 1.2) comprises of two silica-oxygen tetrahedral sheets sandwiching and aluminum or magnesium octahedral sheets (Ismadji *et al.*, 2015). Magnesium or aluminium ions are octahedrally co-ordinated to six oxygen or hydroxyls.

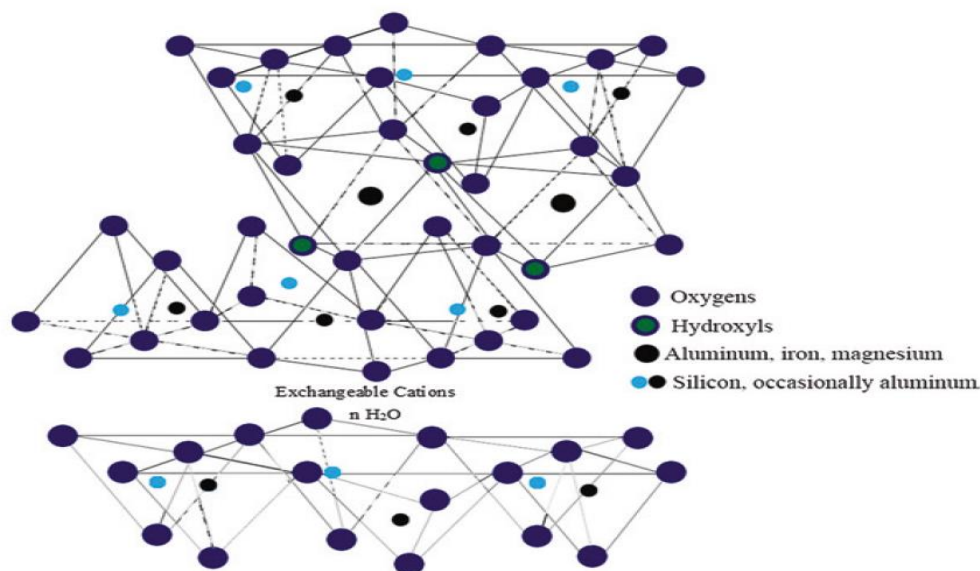


**Figure 1.2: Structure of montmorillonite clay**(Ismadji *et al.*, 2015)

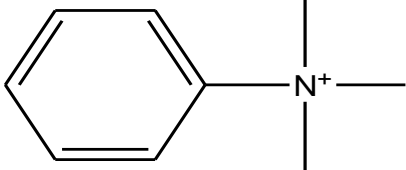
The replacement of silicon by aluminium in the tetrahedral layer makes the layers negatively charged. This makes cations like  $\text{Na}^+$ ,  $\text{K}^+$  and  $\text{Ca}^{2+}$  and  $\text{Mg}^{2+}$  to get attracted to the layers surface to neutralize the negative charges (El-Messabeh-Ouali *et al.*, 2013). Clay formulations have been suggested as the best pesticide carriers due to their sustainability and are economically viable (Celis *et al.*, 2007). The formulations reduce photo degradation, leaching and volatilization thus solving environmental and economical problems (Lagaly *et al.*, 2006).

#### 1.4 Organo clays synthesis and their applications

Clay minerals are negatively charged and hydrophilic thus cationic and highly polar neutral pesticides strongly adsorb on their surface. However, for hydrophobic pesticides adsorption, surface modification using organic cations like quaternary ammonium salts is required resulting to formation of organo clays. This increases clay efficiencies by replacing the existing exchangeable inorganic cations present in the clay gallery spaces with these organic cations to yield hydrophobic organo clays (Celis *et al.*, 2010; Celis *et al.*, 2007). The selection of the cations can be based on the presence of diverse functional groups in the structure which is expected to influence the active ingredient sorption (Gamiz *et al.*, 2010). The length of the alkyl chain is responsible for arrangement of the intercalated organic cation in the organo clay. Short alkyl organic cation chain forms monolayer while long alkyl organic cation chain forms bilayers, pseudo-trimolecular arrangement or paraffin complexes (Paiva *et al.*, 2008). Some of these organic cations are given in Table 1.1.

**Table 1.1: Some selected organic cations** (Aroke *et al.*, 2008)

Name	Abbrev	Structure
Octadecyltrimethylammonium	ODTMA <sup>+</sup>	
Trimethylphenyl	TMPA <sup>+</sup>	

Ammonium		
Hexadecyltrimethyl Ammonium	HDTMA <sup>+</sup>	

### 1.5 Cation exchange capacity

Cation exchange capacity (CEC) is a characteristic property of clay which involves capacity of clay soil to hold cations by electrostatic forces which is expressed as milliequivalent of positive charge per 100g of dry soil (meq/ 100 g) or centimol positive charge per kg of dry soil (cmol<sub>(+)</sub>/kg). The CEC sites are mainly found on clay minerals and organic matter surfaces and can be calculated from levels of Ca<sup>2+</sup>, Mg<sup>2+</sup>, Na<sup>+</sup> and K<sup>+</sup> cations. This is because these cations have the ability of being exchanged for another positively charged ion from the clay minerals surfaces. The choice of the methods for the determination of CEC in clay soils can be based on time of analysis, degree of reliability or the cost of the operation. These methods includes; cation exchange methods using barium, copper or magnesium, classical methods by titrations, use of radioisotopes and ammonium acetate method. Ammonium acetate method of Lewis (1994) is the most widely used of them all as it is very effective on clay and sandy soils, fast, reliable and of low cost thus allowing analysis of large number of samples in a single sequence (Aprile and Lorandi, 2012).

## **1.6 Characterization of clays**

The clay structure and organo-clays can be characterized to determine the functional groups using Fourier Transform Infrared (FT-IR) Spectroscopy and X-ray Diffractometry (XRD). The FT-IR and XRD techniques that were used in this study are discussed in the following subsections.

### **1.6.1 Fourier transform infrared (FT-IR) Spectroscopy**

This technique is used to obtain an infrared spectrum of absorption of clay materials. The mid-infrared region of the FT-IR spectrum is  $4000-400\text{cm}^{-1}$  which contained fundamental information about framework vibrations of siliceous material  $[\text{Si}(\text{Al})\text{O}_4]$ . According to Nayak and Singh (2007), the FT-IR studies helps in the identification of the various forms of minerals which may be coupled vibrations due to presence of various constituents which absorb at different frequencies. FT-IR absorption bands are tentatively assigned to known compounds by comparing them with the published literature helping in their identification. FT-IR mainly compliments X-ray Diffraction (XRD) analytical technique in investigating clays and its minerals by giving information about the isomorphous substituent's nature and distinct molecular water from constitutional hydroxyls. For instance, in clays, the OH stretching vibrations of structural hydroxyl groups is observed at  $3626\text{ cm}^{-1}$ , Si-O stretching of cristobalite at  $1067\text{ cm}^{-1}$ , Al-OH stretching at  $918\text{ cm}^{-1}$  and Al-O-Si deformation at  $529\text{ cm}^{-1}$ . This technique is very common, economical and the clay spectrums can easily be obtained (Majedove 2003).

FT-IR operates by passing the infra-red radiations through a sample. Some of the infrared radiations are absorbed by the sample and some of it is passed through (transmitted). The resulting transmittance represents the molecular absorption and transmission, thus creating a molecular fingerprint of the sample. Each fingerprint has unique molecular structures and unique infrared spectrum.

### 1.6.2 X-ray diffractometry

The X-ray Diffraction (XRD) is one of the most powerful characterization tool used for identifying crystalline minerals present in clay as it offers information about the basal spacing, texture and structural geometry in clay and thus is a technique basically used for mineral analysis (Ravisankar *et al.*, 2010). The XRD technique distinguishes the different types of clays deriving information about their structure composition and is thus the best analytical method as it is accurate, inexpensive, reliable, rapid and non-destructive (Oumabady *et al.*, 2014).

It mainly involves X-rays emissions from the source and consequent X-ray scattering by the electrons of the atoms present in clay sample. The X-rays scattered by different atoms results to diffracted beams which are in turn used to determine the d-spacing in the clay crystals. Each different mineral has distinct d-spacing which are used to identify the minerals. All crystalline minerals in a sample can be identified from one XRD scan. The diffraction patterns (Figure 1.3) can be described by Bragg's law Equation 1:

$$n \lambda = 2 d \sin \theta \dots\dots\dots 1$$

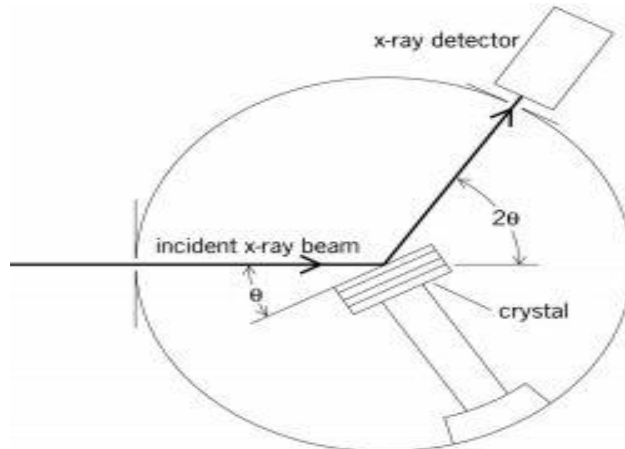


**Figure1.3: Schematic diagram illustrating XRD diffraction (Wanyika, 2012)**

Where integer n is the order of diffraction beam,  $\lambda$  is the wavelength of the incident x-ray beam, d is the distance between atoms (d-spacing) and  $\theta$  is the angle of incidence of the X-ray beam. Known values of  $\lambda$  and  $\theta$  are used to calculate the d-spacing. The d-spacing generated in an x-ray scan provides unique fingerprint of the minerals present in

clay sample and on comparison with standard reference pattern his helps in their identification.

The XRD results thus can give information about the configuration of the surfactant intercalated whether monolayer, bilayer or even paraffin layer. The change in the basal spacing of the clays and organo clays indicates organic cations intercalation in clay layers (Kathleen, 2000). However, XRD does not provide detailed information about the intercalated organic cations and hence FT-IR technique is a complimentary tool (Zhu *et al.*, 2005).

### 1.6.3 X-Ray Florescence

X-ray florescence spectrometry (XRFS) is a suitable method for chemical analysis of clays. XRFS method is fast, accurate and non-destructive and the range of its application includes metals, cement, oil, polymers as well as environmental and waste materials analysis (Neuwirthova *et al.*, 2012). XRF works by dislodging lower energy electrons with X-ray beams from a source. The excited lower energy orbital are replaced by electrons from higher energy orbital, releasing a characteristic energy of the type of the atom present. XRF then interprets these energy signals and also calculates the elemental concentrations.

### 1.7 Adsorption isotherms

The maximum adsorption capacities were calculated by fitting the experimental data from section 2.5.4 in Langmuir and Freundlich isotherms (Patil and Shrivastava, 2010).Langmuir isotherm equation2 is linearly represented as follows:

$$\frac{C_e}{Q_e} = \frac{1}{b} Q_0 + \frac{C_e}{Q_0} \dots\dots\dots 2$$

Where  $Q_e$  is the total PFE uptake (mg/g),  $C_e$  is the PFE equilibrium concentration while  $Q_0$  and  $b$  are Langmuir constants. Langmuir plots of  $C_e/Q_e$  versus  $C_e$  determined  $Q_0$  and

b from slope and intercept respectively. Freundlich Equation 3 is linearly represented as follows:

$$\text{Log } Q_e = \text{Log } K_f + \frac{1}{n} \text{Log } C_e \dots\dots\dots 3$$

Where  $Q_e$  and  $C_e$  have the same meaning as in Langmuir equation while  $K_f$  and  $1/n$  are Freundlich constants. Freundlich plots of  $\text{Log } Q_e$  versus  $\text{Log } C_e$  determined  $Q_0$  and  $b$  from slope and intercept respectively.

### 1.7.1 Kinetic models of sorption

Data from section 2.5.3 was fitted in pseudo-first order and pseudo-second order kinetic models as described by (Pavlovic *et al.*, 2014). The linearized pseudo first-order kinetic model Equation 4 is represented as follows:

$$\text{Log } (Q_e - Q_t) = \text{Log } Q_e - \frac{K_1}{2.303} t \dots\dots\dots 4$$

Where  $Q_e$  and  $Q_t$  are the amount of PFE sorbed on the different clay materials ( $\mu\text{g}/\text{mL}$ ) at saturation and at time  $t$  ( $\mu\text{g}/\text{g}$ ) (Veli and Alyuz, 2007) while  $K_1$  is the pseudo-first order kinetics rate constant. Plots of  $\log (Q_e - Q_t)$  versus  $t$  were used to determine the rate constant,  $K_1$  and correlation coefficient. Pseudo second order kinetics model linearized form Equation 5 is given as follows:

$$\frac{t}{qt} = \frac{1}{K_2 (q_e)^2} + \frac{1}{q_e} \cdot t \dots\dots\dots 5$$

Where  $Q_e$  and  $Q_t$  are as described above while  $K_2$  is the pseudo-second order kinetics (Pavlovic *et al.*, 2014). Straight lines of  $t/Q_t$  versus  $t$  were used to determine the rate constant,  $K_2$ .

### 1.8 Storage of cereals

Maize is a staple food in Kenya and Africa at large, which is usually stored to provide a major food security and planting seeds (Mulungu *et al.*, 2007). Maize is ranked third after wheat and rice in terms of leading crop production in the world. It is a high yielding crop, easy to process and cheaper to produce than any other cereal in the world

(Muzemu *et al.*, 2013). Importance of maize increases rapidly as it is used as food for human and livestock, poultry and industrial raw materials. Thus sustainable production and preservation of maize in future is very important for food security (Parimala and Maheswari, 2013).

Major threats to already harvested and stored maize grains despite high plant yields are the *Sitophilus oryzae* Linnaeus, *Sitophilus zeamais* Motschulsky, *Tribolium castaneum* Herbst and *Rhyzopertha dominica* Fabricius pests. *Sitophilus zeamais* Motschulsky (maize weevils) is the most predominant and destructive of them all (Ngamo *et al.*, 2015). The damage results directly in loss of maize grain quantity and quality reducing the aesthetic and market value, germination ability and nutritional value.

Synthetic pesticides have been used in the control of these pests, but due to their high cost, increasing pest resistance and environmental pollution, the use of alternative control measures are required (Muzemu *et al.*, 2013). According to Gadzirayi *et al.*, (2006), varieties of botanicals are used by farmers in control of these pests. This is because they are less toxic, readily available and effective in these pests control (Asawalan *et al.*, 2006); Belmain *et al.*, 2001); Issa *et al.*, 2001); Wanyika *et al.*, 2009). If sufficiently exploited botanical pesticides can play a major role in reduced health risks, crop losses to pests and environmental pollution (Muzemu *et al.*, 2013).

### **1.9 Botanical control of Cereals**

The maize weevils, *Sitophilus zeamais* Motschulsky is a major pest of stored maize grains. The destructive effect of these weevils has been subdued by synthetic pesticides (Ileke and Oni, 2011). There are many problems with synthetic insecticides including; high persistence, pest resistance, lethal effects on non-target organisms and direct toxicity to users. Currently, attention is being given to use of botanical pesticides as maize protectant (Adedire *et al.*, 2011). Plant materials that are environmental friendly, inexpensive and anti-feedants needs to be exploited as suitable alternatives to synthetic

pesticides (Akunne *et al.*, 2013). Botanical pesticides have been extensively used on agricultural use but very limited extent on insect pests of stored products (Ufele *et al.*, 2013).

### **1.10 Statement of the problem**

Pyrethrum flower extracts are preferred compared to synthetic pesticide use in agricultural pests' control. The advantages of pyrethrum flower extracts pesticides over synthetic pesticides is their rapid target insect control, lack of persistence and bioaccumulation in the environment, low toxicity to both humans and birds. They also have selective toxicity and no beneficial insects are affected, cheap and safe in manufacturing and no harmful residues left in food products. Despite the many advantages, they have a major challenge of photo degradation on UV light exposure reducing their efficacy and thus limited to indoor application use only.

### **1.11 Justification**

Pyrethrum is an important crop in Kenya. Pyrethrum extracts have rapid target insect control, biodegradable, low toxicity to both humans and birds. They also have selective toxicity and no beneficial insects are affected. Most of the pyrethrum flower extracts are sold from Kenya as raw and not the formulated pesticide and thus there is importation of synthetic pesticides. This thus calls for formulation of the effective pyrethrum flower extracts. Clays are natural environmental friendly materials which are locally available. Photo-stabilized PFE-organo-clay would result in formulation of an environmental friendly pesticide which would entirely increase food security and this would entirely boost the Kenya's and global economy.

## **1.12 Hypothesis**

The PFE are not photo stabilized on intercalation in montmorillonite clay gallery space.

## **1.13 Objectives**

### **1.13.1 General Objective**

To investigate photo-stabilization of PFE by intercalation in montmorillonite (MMT) clay.

### **1.13.2 Specific objectives**

- (i) To characterize raw and modified locally available montmorillonite (MMT) clay mineral using FT-IR and XRD techniques
- (ii) To investigate the optimal parameters responsible for sorption of PFEs into clay materials
- (iii) To load the PFE into MMT modified clay gallery space and characterize the product using TXRF, CEC, XRD and FT-IR techniques.
- (iv) To expose the products to UV radiations, monitor their degradation and conduct bioassay tests using these products on maize weevils (*Sitophilus zeamais*)

## **1.14 Significance of the study**

Natural pyrethrum flower extract are botanical pesticides that controls a wide range of pests in agricultural sector. However, their use is limited to indoor applications only due to their photo-labile nature. There is thus a need to photo-stabilize the pesticide in order to increase its effectiveness.

### **1.15 Scope and Limitations**

The study involved characterization of the locally available clays in order to obtain MMT clay. The organic cations would then be intercalated and characterization of the organo clays would then follow. Loading of the pyrethrins in the organo clay, characterization and accelerated stability tests followed to assess the photo stabilization effect of the pyrethrins in clay. Effectiveness of the pyrethrins organo clay composites was assessed using bioassay tests on maize weevils. The limitations of the study involved lack of availability of the equipments for sample analysis. For complex analysis using machines like TEM/SEM, they are not locally available. Moreover, data analysis software are very difficult to access. Finances for students' upkeep, sample analysis, purchase of reagents are a major challenge in the research world. The highlighted issues if well addressed would be a great milestone to the research.

## CHAPTER TWO

### 2.0 MATERIALS AND METHODS

#### 2.1 Research designs

Procedures for the research project involved both qualitative and quantitative analysis as outlined in the following subsections.

#### 2.2 Solvents and reagents

Solvents and reagents used throughout this research project were of high purity. Pyrethrum pale extract containing 50% pyrethrins was acquired from Sigma-Aldrich. HDTMA, TMPA, n-Hexane (analar), acetonitrile (HPLC) and absolute ethanol (analar) were purchased from Sigma-Aldrich, U.K. (99% purity).

#### 2.3 Preparation of standards

The standard solutions of the exchangeable cations;  $K^+$ ,  $Na^+$ ,  $Ca^{2+}$  and  $Mg^{2+}$  were first prepared as described: potassium, sodium, calcium and magnesium standard solutions of 100 ppm were prepared by dissolving 0.022 g of  $K_2SO_4$ , 0.0597 g of NaOH, 0.0244 g of  $Ca(NO_3)_2$  and 0.02 g of  $MgSO_4$  in 100 mL of distilled water.

#### 2.4 Collection of clay samples and pretreatment

Four composite clay samples denoted A, B, C and D were collected from Jomo Kenyatta University of Agriculture and Technology (JKUAT), Nairobi, Kenya from four different

locations; farm, piggery, outside swimming pool and JKUAT main gate areas respectively (Figure 2.1).

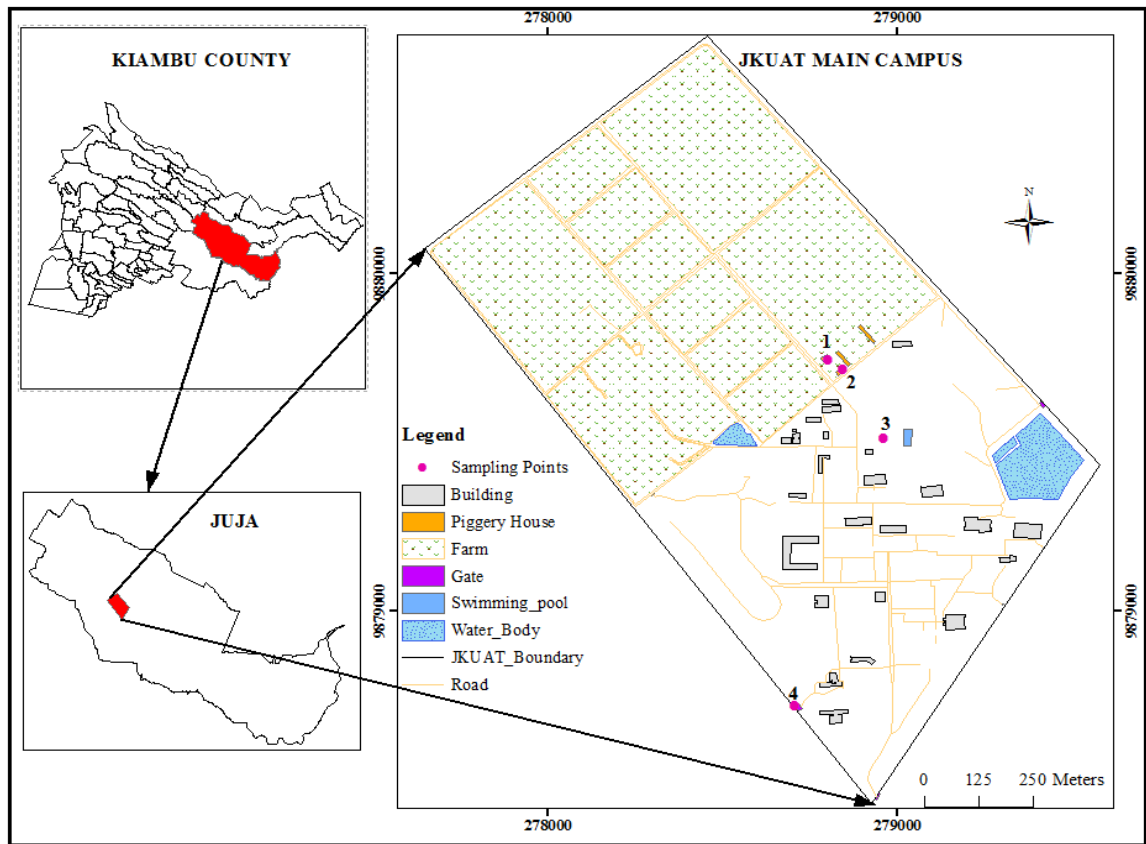


**Figure 2.1: Sample collection area**

The vegetation was first cleared using a panga and the top soil which was expected to contain organic matter removed to about  $10 \pm 1.0$  cm. Samples ( $20 \pm 1.0$  kg) were collected through digging  $20 \pm 2.0$  cm deep holes, they were sieved through 2 mm mesh size, put in plastic paper bags, carried to the laboratory and kept at room temperatures for further analysis.

The clay samples were purified using methods described by James *et al.*, (2008). In summary, the following methods were followed; the sample was broken into smaller lumps and larger particles consisting of pebbles, leaves and roots removed. Coarse particles and stones were removed by sieving through 2mm mesh size. The resultant

clay sample was then dried in an oven model no. 01410.CI Brisbane, Australia, to about 150°C to remove moisture and volatile organics. The sample was milled and passed through 420µm mesh size. One part of the resultant milled sample was purified further by dispersing 100g in 1L of 10% hydrogen peroxide in order to remove any soil organic matter present. The suspension was stirred and allowed to stand for 3hours. The clear suspension was decanted and the remaining clay was re-suspended in 1L 0.5M sodium hydroxide and stirred using a magnetic stirrer (100 rpm) for 45 minutes. The resulting solution was decanted and the remaining clay left to dry at 105°C in the oven for 24hours. The other part was used without further purification.

## **2.5 Isolation of clays**

Clay particles were isolated from the purified clay using the following procedure: A sample (100 g) was dissolved in 1 L of distilled water. The solution was stirred using a magnetic stirrer for 4hours and left to stand for 12 hours. The supernatant was pipetted out and centrifuged at 6000 rpm for 20 minutes to obtain the  $\leq 2\mu\text{m}$  particle sizes. The sediment was scooped out using a spatula, dried in the oven at 105 °C for 3 hours and crushed into smaller particles using motor and pestle. The sample was allowed to pass through 200 µm mesh size.

## **2.6 Characterization of the clays**

### **2.6.1 Elemental analysis using total x-ray fluorescence spectrometry (TXRF)**

The Fe, Ca, K and Mn contents of the clay samples were determined using S2 PICOFOX TXRF Spectrometer. The samples were prepared by digestion method which entailed weighing 1.00 g of the clay sample and transferring it into 250 mL conical flask, 10 mL of 1:1 HNO<sub>3</sub> was added, mixed and covered with a watch glass. The mixture was heated to 90 °C and refluxed for 15 minutes without boiling. It was then cooled and 5

mL of concentrated HNO<sub>3</sub> was added, covered and refluxed for 30 minutes. Brown fumes were generated, which indicated oxidation of the clay sample by HNO<sub>3</sub>. The step of addition of 5mL of concentrated HNO<sub>3</sub> was repeated until no further brown fumes were given off indicating complete reaction.

The glass bottles that were used in the experiment were first cleaned by immersing them in 1.5 % concentrated HNO<sub>3</sub> solution overnight and rinsed with dilute nitric acid solution. The rinsing solutions were analyzed for any trace impurity. In case impurities were found, further cleaning was done. The clay sample solutions were subjected to TXRF to analyze the chemical composition or elements present. The quartz sample support were also cleaned with 1.5 % concentrated HNO<sub>3</sub> and checked for contamination by acquiring the TXRF spectrum before the sample deposition.

All sample standards were diluted with 1.5 % concentrated HNO<sub>3</sub>. Clay sample solutions (5mL) were taken separately into the earlier cleaned glass bottles. Ga internal standard solution (50 µl of 5 µg/mL) was mixed with 5mL of clay sample solutions. Solutions (20µl) were deposited ten times independently on six quartz sample supports so that 200µl of the clay sample solutions were deposited and dried on IR lamp. The TXRF spectrum for each sample was recorded for 20 minutes (Misra and Dhara, 2011).

### **2.6.2 Determination of basal spacing and crystallite size**

The clays were subjected to further purification following the method of Yunfei (2007). In summary, the following procedures were followed: Iron oxide impurities were removed by treating clay (50 g) with sodium citrate reagent made by dissolving 15.06 g of sodium citrate in 200 mL of distilled water followed by addition of 1.50 g of NaHCO<sub>3</sub> and 14.00 g of NaCl. The mixture was heated to 80 °C for 30 minutes. Then, the solution was centrifuged at 600 rpm for 20 minutes and the supernatant discarded. Lastly, the clay was washed three times with 1M NaCl. Carbonate impurities were removed by suspending the clay sample from the previous procedure in 1 L aqueous solution

containing 136g sodium acetate at pH 4.8 followed by washing thrice with 1 M NaCl. In order to remove organic matter, the dry clay sample was re-suspended in 30% H<sub>2</sub>O<sub>2</sub> and heated to 80 °C for 30 minutes. The suspension was centrifuged at 600 rpm for 20 minutes. Excess H<sub>2</sub>O<sub>2</sub> was removed by washing the sample three times with distilled water followed by centrifugation at 6000 rpm for 20 minutes and oven drying at 105 °C. Finally, a part of the sample was treated by exposure to vapour of ethylene glycol and dried at 60 °C in the oven (Lab Manual, 2008) while the other part was heated in the oven at a temperature of 550 °C for 40 minutes in order to collapse any expandable layers (Moore and Reynolds, 1989). The treated samples were analyzed by X-ray diffractometer as described by Gueganet *al.*, (2009).

The X-ray diffractometer measurements were done with Cu-K $\alpha$  radiation of wavelength 1.5418 Å on Rigaku Manniflex II Desktop operating at 40 KV and 30 mA. The scan range was 1° through 45 ° at a scanning rate of 1°/ min with a step size of 0.04°. Diffraction peaks of the raw clay sample were compared with those of standard clay materials. The sample crystallite size of the clay was measured using Debye-Scherrer's equation from the XRD peaks expressed in Equation 6:

$$D = K \left\{ \frac{\lambda}{\beta \cos \theta} \right\} \dots \dots \dots 6$$

Where D is Crystallite size, K is 0.89 (constant),  $\lambda$  is X-ray wavelength 1.540562 (Å),  $\beta$  is peak width at half maximum,  $\theta$  = scattering angle (Hassani *et al.*, 2015).

**2.6.3 Determination of cation exchange capacity(CEC) of clay**

The CEC of clay was determined using ammonium acetate method (Mehlich, 1938). Serial dilutions in the range of 0.10-1.50 ppm for potassium and sodium, 0.15-5 ppm for calcium and 0.10-1.50 ppm for magnesium were made in triplicates. In all the standards, about 1.00mL of 5% La<sub>2</sub>O<sub>3</sub> solution was added and solution shaken for 15 minutes. Lanthanum oxide solution (5%) was prepared by dissolving 50gLa<sub>2</sub>O<sub>3</sub>in 100mL concentrated Hydrochloric acid, the mixture was cooled and diluted to 1L with distilled water. Atomic absorption spectrophotometer (AAS), Buck Scientific model no. 210VP

was used to determine magnesium and calcium. FES Buck Scientific model no. AFP 100 was used for potassium and sodium analysis. The concentrations of the respective cations in the different samples were determined by interpolation using regression equations of best lines of fit.

Ammonium acetate (1M, pH 7) was prepared by adding 57 mL of glacial acetic acid and 68 mL of concentrated ammonium hydroxide to 800 mL of distilled water in a 1 L volumetric flask. The solution was allowed to cool, pH adjusted to 7.0 using 3 M acetic acid and diluted to 1L mark using distilled water. Each clay sample (2.5 g) was put in 250 mL beaker and 25 mL ammonium acetate solution added. The solution was shaken for 30 minutes and was then filtered through a Whatman filter paper no. 1. Each clay sample solution (100  $\mu$ L) was pipetted and transferred to 50 mL volumetric flask.  $\text{La}_2\text{O}_3$  (2 mL of 5 %) solution was added and was topped with distilled water. The samples were analyzed for  $\text{K}^+$  &  $\text{Na}^+$  using FES and  $\text{Mg}^{2+}$  &  $\text{Ca}^{2+}$  using AAS.

#### **2.6.4 Functional groups determination using fourier transform-infrared (FT-IR) spectroscopy**

The sample spectra were acquired using SHIMADZU FT-IR spectrophotometer model number 8400 in the range of 400 – 4000 $\text{cm}^{-1}$ . The sample was prepared as a KBr disc by mixing 0.01mg of air dried clay with 0.25 mg dried potassium bromide (KBr).

#### **2.6.5 UV-Visible spectrophotometry for determination of transitional groups**

About 1.0 g of the clay sample was mixed with 10 mL of concentrated nitric acid and refluxed at 90  $^{\circ}\text{C}$  for 15 minutes. Additional 5 mL portions of concentrated nitric acid were added to the cooled sample and refluxed at 95  $^{\circ}\text{C}$  for 30 minutes. This stage was repeated until more addition did not produce brown fumes. The solution was then refluxed for 2 hours. Once the solution was cooled to room temperature, 2 mL distilled water and 3 mL of 30 %  $\text{H}_2\text{O}_2$  were added and the solution warmed until effervescence ceased. Additional 1mL portions of hydrogen peroxide were added followed by heating

until effervescence became negligible. The solution was then refluxed for 30 minutes and allowed to cool. Concentrated Hydrochloric acid (10 mL) was added followed by 15 minutes of refluxing. After the solutions cooled, it was filtered through Whatman filter paper number 1 into 100 mL volumetric flask and was made to mark with distilled water.

The sample solution was diluted in the ratio 1:50 (v/v) portions of sample into distilled water respectively. One of the cuvettes was filled with distilled water (blank) and the other was filled with the diluted sample solution. The spectra were acquired using the SHIMADZU UV/Vis Spectrophotometer model no. 1800 with the scan range of 200-700 nm and the results were analyzed.

## **2.7 Preparation of organo clay**

The clay with the highest CEC was modified with organic cations; hexadecyltrimethylammonium bromide (HDTMA) and trimethylphenylammonium bromide (TMPA). Hexadecyltrimethylammonium bromide (2.0 g) was dissolved in 50 mL of a mixture of 1:1 v/v distilled water and ethanol (Musleh *et al.*, 2014). Clay sample (2.0 g) was added to the solution and stirred using magnetic stirrer at 250rpm for 12 hours to provide sufficient contact time between surfactant solution and the clay sample. The mixture was then centrifuged at 6000 rpm for 20 minutes to remove the sediment. The clay sediments were washed twice with; (a) 50 mL ethanol- distilled water in the ratio 1:1 and (b) in 97 % ethanol. The washed out solids were separated by centrifugation at 6000 rpm for 20 minutes and sediment dried at 80 °C in an oven to a constant mass. The sample was crushed to smaller particles using motor and pestle and allowed to pass through 200 µm mesh size.

Same procedure was followed with trimethylphenylammonium bromide (2.00 g) as above instead of hexadecyltrimethylammonium bromide (HDTMA). The organo-clays

(HDTMA-clay and TMPA-clay) were analyzed by FT-IR spectrophotometry and X-ray diffractometry.

## 2.8 Determination of sorption kinetics of PFE into clay materials

The optimal parameters on the intercalation of PFE into clay materials were investigated using SHIMADZU UV/Vis Spectrophotometer and acetonitrile was used as a blank at 225 nm. Stock solution of the pyrethrum flower extracts (PFE) was made by dissolving 2.0 g PFE (50% active ingredient) in 1 L acetonitrile to make 1000 µg/mL. Using this as stock solution, five serial dilutions in the range of 0.5- 3.5 µg/mL were made in triplicates. A calibration curve was constructed by plotting absorbance against concentration (Dessalgane *et al.*, 2011). The sorption experiment was carried out in triplicates.

The sorption capacity was calculated using the Equation 7:

$$\% \text{ sorption capacity} = \left( \frac{C_i - C_f}{C_i} \right) \times 100 \% \dots\dots\dots 7$$

Where  $C_i$  = initial PFE concentration (µg/mL);  $C_f$ =final concentration (µg/mL).

The adsorption capacity,  $q$ , was calculated based on the mass balance principle according to equation 8:

$$Q_e = \frac{C_i - C_f}{m} \times V \dots\dots\dots 8$$

$Q_e$  = Sorption capacity (amount of PFE molecules adsorbed per unit mass of dry adsorbent in mg/g);  $V$  = volume of the reaction mixture (mL);  $m$  = mass of adsorbent used (mg);  $C_i$  = initial concentration (µg/mL) and  $C_f$  = final concentration (µg/mL).

### 2.8.1 Determination of pH

PFE sorption was monitored the pH range 3-7 using hydrochloric acid to adjust. All pH measurements were made using JENWAY model 210 pH meter. Each sample (unmodified, HDTMA and TMPA modified Clay, 0.2 mg) was dispersed in 50 mL solution containing 3.5 µg/mL PFE, stirred using automated rotary shaker at 100 rpm for 60 minutes. The mixture was centrifuged at 6000 rpm for 20 minutes and the supernatant

analyzed using UV/Visible spectrophotometry. The difference in initial and final absorbance in the supernatant was taken to be the amount of PFE sorbed in clay matrix (Kurkova *et al.*, 2000).

### **2.8.2 Effect of temperature**

Temperatures were varied from 25-65 °C using an automated rotary shaker at 100 rpm at PFE initial concentration of 3.5 µg/mL (Namasivayam and Sureshkuar, 2007). Solutions were withdrawn after 60minutes, centrifuged at 6000 rpm for 20 minutes and the absorbance of PFE concentration remaining in the supernatant measured using UV-Vis Spectrometer ( $\lambda_{max} = 225\text{nm}$ ). The difference in initial and final absorbance in the supernatant was taken to be the amount of PFE sorbed in the clay matrix (Kurkova *et al.*, 2000).

### **2.8.3 Determination of initial concentration and contact time**

The experiment was carried out at optimum pH and temperature as determined in sections 2.5.1 and 2.5.2. Solution (50 mL) containing initial concentration of 0.5, 1, 1.5, 2.0, 2.5 or 3.5 µg/mL PFE was added to 0.2 mg of each clay material and the solutions stirred using automated rotary shaker at 100 rpm. Supernatant was monitored at various times (10, 30, 60, 90, 120 minutes), centrifuged at 6000 rpm for 20 minutes and the PFE concentration remaining in the supernatant was measured using UV-Vis Spectrophotometry. The difference in initial and final absorbance in the supernatant was taken to be the amount of PFE sorbed in clay matrix.

### **2.8.4 Effect of sorbent dosage**

Varying mass of clay, that is, 0.1, 0.2, 0.25, 0.5, 1.0 and 1.5 g were investigated for PFE sorption capacity at an initial concentration of 3.5 µg/mL, optimal pH, temperature and contact time and solution stirred using automated rotary shaker at 100 rpm after 120 minutes. Solutions (50 mL) were withdrawn, centrifuged at 6000 rpm for 20 minutes and

absorbance was recorded using UV/Visible spectrophotometry. The difference in initial and final absorbance in the supernatant was taken to be the amount sorbed.

## **2.9 Loading of PFE into clay materials**

Pyrethrins (3.5 µg/mL) dissolved in 50 mL acetonitrile were added to clay samples (1.0 g). The solution was stirred using automated rotary shaker for 120 minutes at 45 °C and pH 3 for both the Un-modified and TMPA modified clay and; pH 5 for HDTMA modified clay at 100 rpm to provide sufficient contact. The mixture was centrifuged at 6000 rpm for 20 minutes. The clay solids were then washed twice with acetonitrile to remove the loosely adsorbed pyrethrins on clay surface as indicated above. The resultant clay sample was crushed to smaller particles using motor and pestle. The sample was allowed to pass through 200 µm mesh size. The PFE-clay composites were characterized by FT-IR spectrophotometry and X-ray diffractometry.

## **2.10 Accelerated photo stability test**

HPLC was used to quantify pyrethrins in the pyrethrum based mixtures. Stability tests analysis for pyrethrum flower extracts were made using 250 mm x 4 mm C 18 with acetonitrile (85 %) and water (15 %) as the mobile phase (Kasaj *et al.*, 1999). The flow rate was 1mL/ min with an injection volume of 10 µL where the PFE were detected at UV absorption of 225 nm. Standard pyrethrum extract containing 1000 µg/ mL pyrethrins was prepared from the 50 % pyrethrins pale extract by dissolving 2.0g of the extract in 1 L of the mobile phase. Calibration standards containing 10 – 180 µg/mL pyrethrins were prepared by serial dilution of the stock solution using the mobile phase. A calibration graph was obtained by plotting the sum of peak areas of the six pyrethrum esters (pyrethrins) against the concentration of the standards. The concentration of pyrethrins in the samples was obtained by interpolation of the best line of fit.

The protective effect of the clays and modified clays on the PFE was confirmed by illuminating PFE clay composites samples with UV light from a UV lamp at 254 nm and 366 nm; and natural sunlight for 4 hours. PFE (0.00848 g), (0.0136 g) and (0.0106 g) were used as control for Un-modified, HDTMA-clay and TMPA-clay respectively. The irradiations were performed in quartz cuvettes (1x1 cm; total volume 3 mL). The distance between the lamps and the cuvettes was 5 cm and temperature was maintained at 25 °C. The PFE initial and final concentration was determined using HPLC as described above.

## **2.11 Bioassay tests on maize weevils using clay samples**

### **2.11.1 *Sitophilus zeamais* motschulsky culture**

Adult maize weevils (*Sitophilus Zeamais* Motschulsky) were collected from naturally infested maize grains from a local market in Thika town. The insects were then reared on clean and un-infested maize grains under laboratory conditions of  $27 \pm 2$  °C. Fine fabric was used to cover the glass jars to prevent weevils' escape and also allowed air circulation (Yankanchi and Gadache, 2010). According to Masiwa (2004), weevils have a minimum life cycle of 28 days at temperature of 27°C in an incubator, so after four weeks the insects were thoroughly sieved and discarded appropriately. The infested and oviposited grain was returned in the incubator at temperatures of 27 °C, and after one week, 20 vigorous, healthy insects were used for the bioassay analysis.

### **2.11.2 Bioassay**

Preliminary experiments were conducted to determine the appropriate dose range of the samples (Okomoda *et al.*, 2013). Each sample (PFE-Clay, PFE-TMPA clay, PFE) was first exposed to sunlight for a period of 4 hours before the experiment was started. Bioassay analysis was carried out by treating clean undamaged maize with pyrethrins loaded clay materials having 75 % active ingredient granular formulation; PFE-Clay,

PFE-TMPA clay, PFE-HDTMA clay in comparison with HDTMA-clay, TMPA-clay, Clay, un-degraded PFE, degraded PFE and untreated maize (control) using 20 maize weevils, at two concentrations levels of 0.1 g and 0.5 g, a method described by Wanyika *et al.*, (2009); Issa *et al.*, (2011) with slight modifications. A completely randomized design was used to arrange the 27 jars used in the experiment, with each treatment being done in triplicates and the insects examined daily (<sup>(a)</sup>Muzemu *et al.*, 2013). Clean maize grains were first sieved through 2.0 mm mesh size to remove any foreign and fluffy materials.

Each sample (PFE-Clay, PFE-TMPA clay, PFE-HDTMA clay, HDTMA-clay, TMPA-clay, Clay, un-degraded PFE, degraded PFE) at two levels of concentration (0.5 g and 1.0 g) corresponding to 2.5 % and 5.0 % w/w concentrations were added to 30 g of the clean maize grain. The mixture was shaken for 30 minutes and put in 250 mL glass jars. Adult maize weevils (20) of mixed sex were introduced and mortality rate observed at 24, 48, 72, 96 and 120 hours in each experiment.

The grains were sieved using 2.0 mm mesh size and the numbers of live and dead pests were counted where they were considered dead if there was no response on gentle touch using faint brush. Maize weevils' percentage mortality rate was calculated using equation 9. Dead insects were discarded. Data obtained was subjected to Analysis of Variance (ANOVA) and significantly different means separation obtained using the least significant difference (LSD) at 5 % level of probability (Ileke and Oni, 2011).

$$\text{Percentage weevil mortality} = \frac{\text{Number of dead weevils}}{\text{Total number of weevils}} \times 100 \dots\dots\dots 9$$

## CHAPTER THREE

### 3.0 RESULTS AND DISCUSSION

#### 3.1 Purification of clays

The clay soil samples were collected from JKUAT farm from four different sites and denoted as A, B, C and D. On sieving through 2.0 mm mesh size, samples A and B yields was high (Figure3.1).

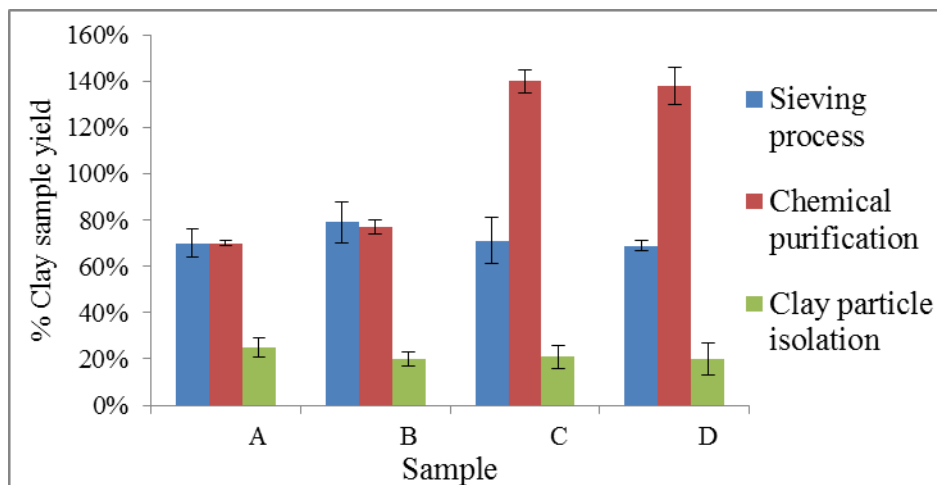


**Figure 3.1: Different clay sample purification methods**

This may be due to the sampling sites being characterized by ploughing activities. Sample D had the lowest yield due to less agricultural activities in the area. During chemical purification stage, there was high rate of effervescence and emission of heat and this method proved to be more effective in the removal of inorganic matter. The yield of these samples increased due to absorption of water. The final process of isolation of  $\leq 2 \mu\text{m}$  clays gave the smallest quantity yield. This was because the sample was initially suspended in distilled water.

### 3.2 Characterization of the clays

This was done using TXRF, FT-IR, UV-Visible, XRD and CEC. The results are presented in the following sub-sections.

#### 3.2.1 TXRF Elemental composition

TXRF results collected showed presence of major and minor elements. Iron (Fe) was the major element which occurred in the range of 30-54 % when expressed as Fe<sub>2</sub>O<sub>3</sub> (Figure 3.2) (appendix 1), while all other elements; K, Ca, Cu, As, Pb, Sr, Mn and Rb occurred as minor elements (Table 3.1).

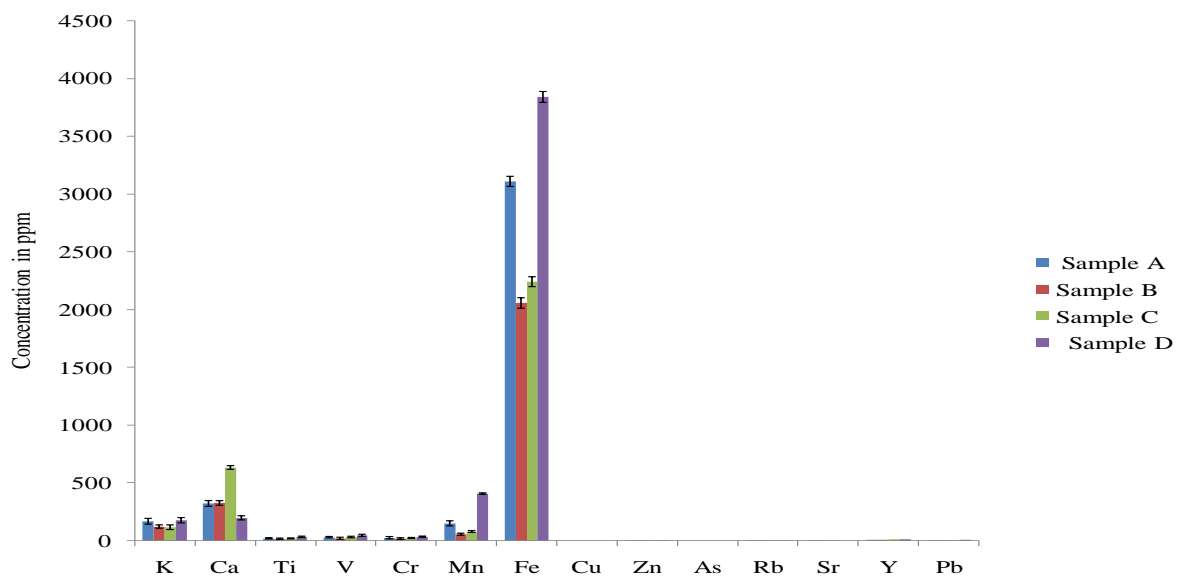


**Figure 3.2: Elemental composition (ppm) of different clay samples**

**Table 3.1: Oxide levels (%) of the clay samples**

	A	B	C	D
Fe <sub>2</sub> O <sub>3</sub>	44.00	30.00	31.00	54.00
CaO	4.10	4.10	7.00	2.40
K <sub>2</sub> O	2.40	2.40	2.40	2.40
MnO	3.10	2.00	1.00	1.00

Montmorillonite clays minerals have complex structures of  $\text{Fe}^{2+}$ ,  $\text{Fe}^{3+}$  and  $\text{Mn}^{2+}$  ions in octahedral sheets embedded with other metal cations like  $\text{Si}^{4+}$  and  $\text{Al}^{3+}$  in the tetrahedral layer. This highest  $\text{Fe}_2\text{O}_3$  percentage in the clay samples signified presence of montmorillonite clay minerals. Potassium and calcium ions occurred in the clay gallery spaces while the other minor elements were embedded in clay structure. The variation between the clay samples may have been due to the different sampling sites. Similar observations were made by Muriithi *et al.*, (2012) and Antoaneta, Alina, & Georgescu (2009).

### 3.2.2 The FT-IR spectra of the clays

After the samples were subjected to FT-IR spectroscopy determination, the spectra were found to have similar vibrational bands characteristics of MMT clay in all the samples (Figure 3.3).

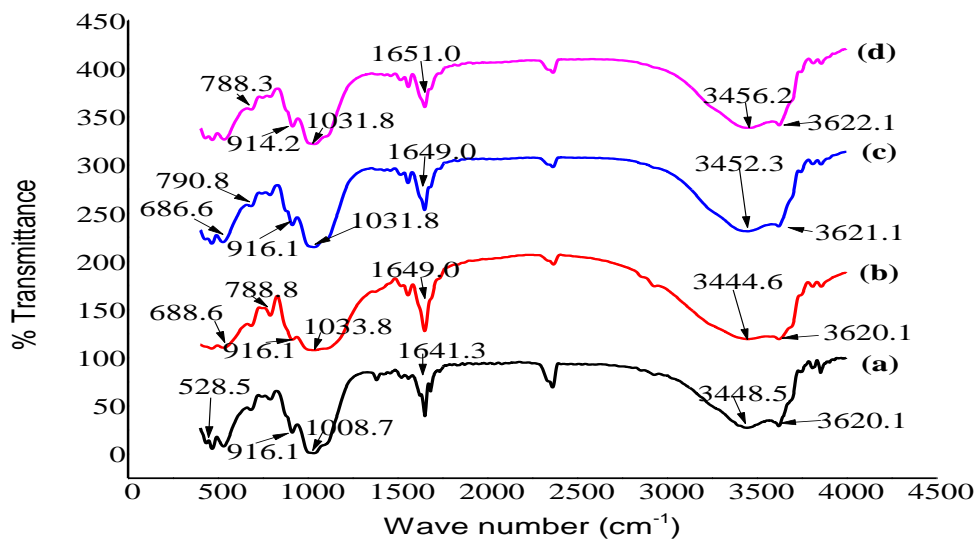


**Figure 3.3: FT-IR spectra of clay samples; (a) A, (b) B, (c) C and (d) D**

The Si-O and Al-OH were the main functional groups observed in the range of  $1000\text{ cm}^{-1}$  and  $500\text{ cm}^{-1}$ . Intensive peaks at  $528.5\text{ cm}^{-1}$  was due to the bending vibrations of Al-O-Si bond while bands at  $914\text{-}916\text{ cm}^{-1}$  corresponded to the Al-OH bending vibrations. The doublet at  $780\text{-}798\text{ cm}^{-1}$  was due to Si-O-Si inter tetrahedral bridging bonds in  $\text{SiO}_2$

and OH deformation bond of gibbsite. Si-O stretching vibrations were observed at around 780-686  $\text{cm}^{-1}$  showing presence of quartz.

Strong bands at around 3620  $\text{cm}^{-1}$  showing presence of hydroxyl linkage while broad band at 450  $\text{cm}^{-1}$  and bands at 1650-1641  $\text{cm}^{-1}$  in the clay spectrum indicated possibility of water of hydration or H-O-H bending of water in the adsorbent due to the hydrous nature of the clay materials. The clay minerals present in the clay samples were mainly K, Na, Ca, Si, Al and O. The results were helpful in identification of the various forms of minerals present in clay. The chemical composition of clay mineral is clearly indicated by the position of the band. The important bands that are needed for identification of montmorillonite clay are at absorption bands at position 1, 2, 7 and 8 (Table 3.2). Similar results were observed by many researchers (Adikary and Wanasinghe, 2012; Hasmukhet *et al.*, 2006; Navratilova *et al.*, 2007; Nayak and Singh, 2007; Saiki and Parthasarathy, 2014 and Thambavani and Kavitha, 2014).

**Table 3.2: The FT-IR absorption bands of different clay samples**

Absorption band position	Theoretical Montmorillonite	Sample Wave numbers (cm <sup>-1</sup> )				Assignments
		A	B	C	D	
1	3630	3620.1	3620.1	3620.1	3622.1	Al/Mg--O-H stretching  (Inter-octahedral)
2	3427	3448.5	3444.6	3452.3	3456.2	H-O-H stretching of structural hydroxyl groups & water
3	1636	1641.3	1649.0	1649.0	1651.0	OH deformation of water
4	-	1558.4	1558.4	1558.4	1558.4	C-N stretching
5	-	1514.0	1519.8	1515.9	1508.2	Aromatic nitrate
6	1065	-	-	-	-	Si-O stretching of quartz in plane vibration
7	1049	1008.7	1033.8	1031.8	1031.8	Si-O stretching
8	918	916.1	916.1	916.1	914.2	Al-Al-OH bending/ deformation
9	-	788.8	790.8	788.8	788.8	Si-O quartz
10	695	-	686.6	686.6	688.5	AlAlOH bending

### 3.2.3 UV-Visible Spectra

The spectra of the UV-Visible sample analysis are shown in Figure 3.4 with the peaks ranging from 200-300 nm.

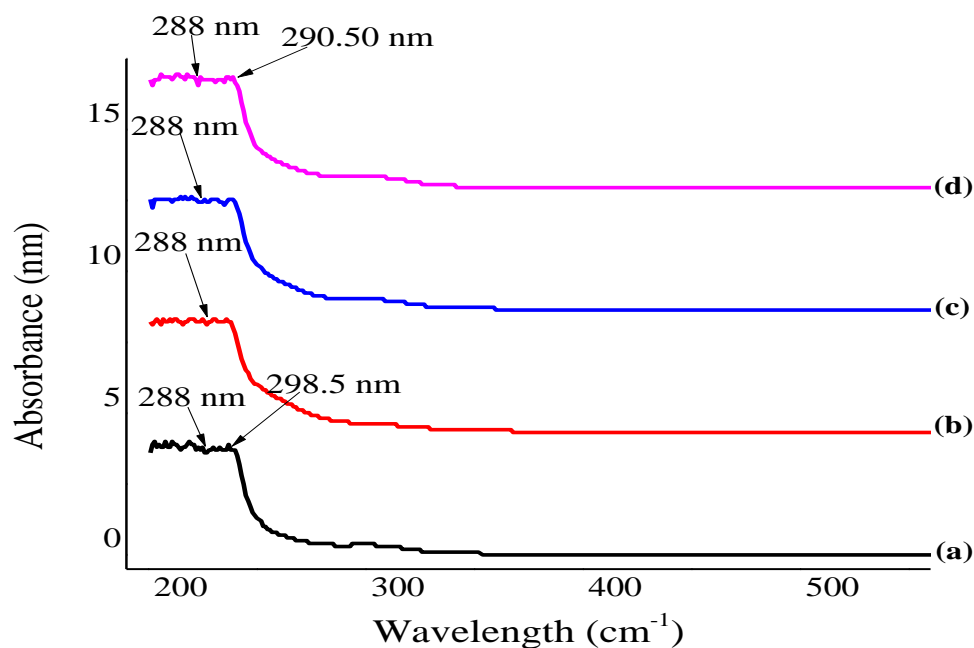


**Figure 3:4: UV-Visible Spectra of: (a) clay A, (b) clay B, (c) clay C and (d) clay D**

This indicated presence of conjugated systems as earlier observed using FT-IR technique. Broad bands were observed in the range of 270-300 nm which can be attributed to montmorillonite clay possessing chromophores that absorbs in this region attributed to the structural conjugation of ketones indicative of quartz as earlier observed in FT-IR results (Cuhna *et al.*, 2009). In sample A, B and C (Figure 3.4), the characteristic bands present at 288 and 236 nm were attributed to sigma-sigma anti-bond transitions of Si-O functional group.

### 3.2.4 The XRD Analysis

XRD was used for qualitative evaluation of the purified clay samples where the d-values were compared with those published in literature. The identification of the clay minerals was accomplished by careful consideration of peak position and intensities in comparison with the spectra from selected powder diffraction data for minerals and powder diffraction file search manual minerals. The analysis was measured in the range

of  $1-45^\circ 2\theta$  and the diffraction patterns were obtained at different clay treatment; **(a)** Ethylene glycol (EG) and **(b)** at high temperatures of  $550^\circ\text{C}$  (Figure 3.5) (appendix 2).

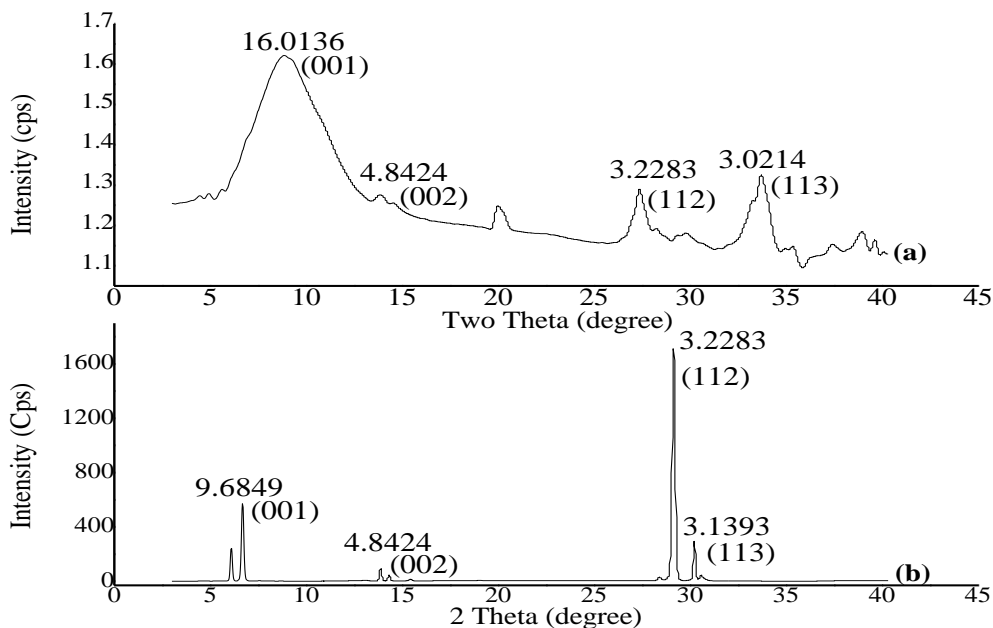


**Figure 3.5: X-ray diffraction patterns of unmodified clay minerals at different sample treatment; (a) treated with Ethylene Glycol and (b) heated at high temperatures of  $550^\circ\text{C}$**

From the preliminary identification of clay minerals responsible for reflections in the zone  $2\theta = 4^\circ$  to  $2\theta = 10^\circ$  it is not possible to point out without the aid of further treatments. However minerals that were expected to occur were:

Chlorite (Mg)	$d = 14 \text{ \AA}$
Chlorite (Fe)	$d = 14 \text{ \AA}$
Swelling Chlorite	$d = 14 \text{ \AA}$
Vermiculite	$d = 14 \text{ \AA}$
Montmorillonite group	$d = 13-18 \text{ \AA}$

On clay treatment with ethylene glycol, the present peaks shifted. Chlorite and Vermiculite minerals do not show any response on glycolation. No mineral other than

montmorillonite minerals undertakes changes on these treatments, and hence all reflections occurring in the zone  $2\theta = 4^\circ$  to  $2\theta = 10^\circ$  were caused by montmorillonite clay minerals (Dafalla and Ali, 1991).

The small and wide angle x-ray diffraction patterns showed diffraction peaks at miller indices (001), (002), (112) and at (113) (h,k,l) indicating a one dimensional (1D) and three dimensional (3D) long range ordering and a hexagonal MMT unit cell. The diffraction peaks of the (001) plane at  $16.0136\text{\AA}$  and (113) plane at  $3.0214\text{\AA}$  appeared on sample treatment with ethylene glycol that are typical of Na/Fe II montmorillonite. The montmorillonite clay d-spacing at  $16.0136\text{\AA}$  indicated that the silicate layer was dioctahedral with aluminium as the cation and the interlayer cation being sodium with its position as a fixed midway between adjacent silicate layers (Viani *et al.*, (2002).

The layer structure is observed to be constant in the region of maxima(001) montmorillonite-glycol treatment and the region of maxima (001) heated montmorillonite Figure 3.5, suggesting that the breadths of the reflection were; (1) measure of particular thickness(mean distance perpendicular to the layers) and thus the number of layers per particles and (2) the position of these maxima were unaffected by the thickness of the particles, overall chemical composition, specific nature of the particle and thus were a measure of thickness of the unit layer. Heat treatment in conjunction with x-ray diffraction measurement is a valuable technique in identification of clay minerals. On heating to high temperatures of  $550^\circ\text{C}$ , the maximum intensity of the (001) peak is at  $9.6849\text{\AA}$  due to phase transformation (Alluminium-hydroxy-montmorillonite to stable oxy-alluminium-montmorillonite) characteristics of dehydrated montmorillonite clay mineral. This peak had the strongest reflection resulting from the greater quantity of MMT clay mineral in the sample. Thus the high temperatures acted as a driving force for the growth of the crystallite sized sample and can be used as crystallite activation energy as observed in Figure3.5. The diffraction peaks occurring at (002) and (112) corresponding to d-spacing of  $4.8424\text{\AA}$  and  $3.2283$

Å respectively appeared on heating due to presence of illite impurities in the sample. Similar results were observed by many researchers. (Bindu and Thomas, 2014, Monshi *et al.*, 2012, Gaber *et al.*, 2013, Njoka *et al.*, 2015, Lugwisha, 2011, Navratilova *et al.*, 2007).

### **3.2.5 CEC of the clays**

Ammonium acetate method for classification of the soil was selected for CEC determination. Respective calibration curves were drawn for the four ions under consideration (Figure 3.6) (appendices 3, 4, 5 and 6).

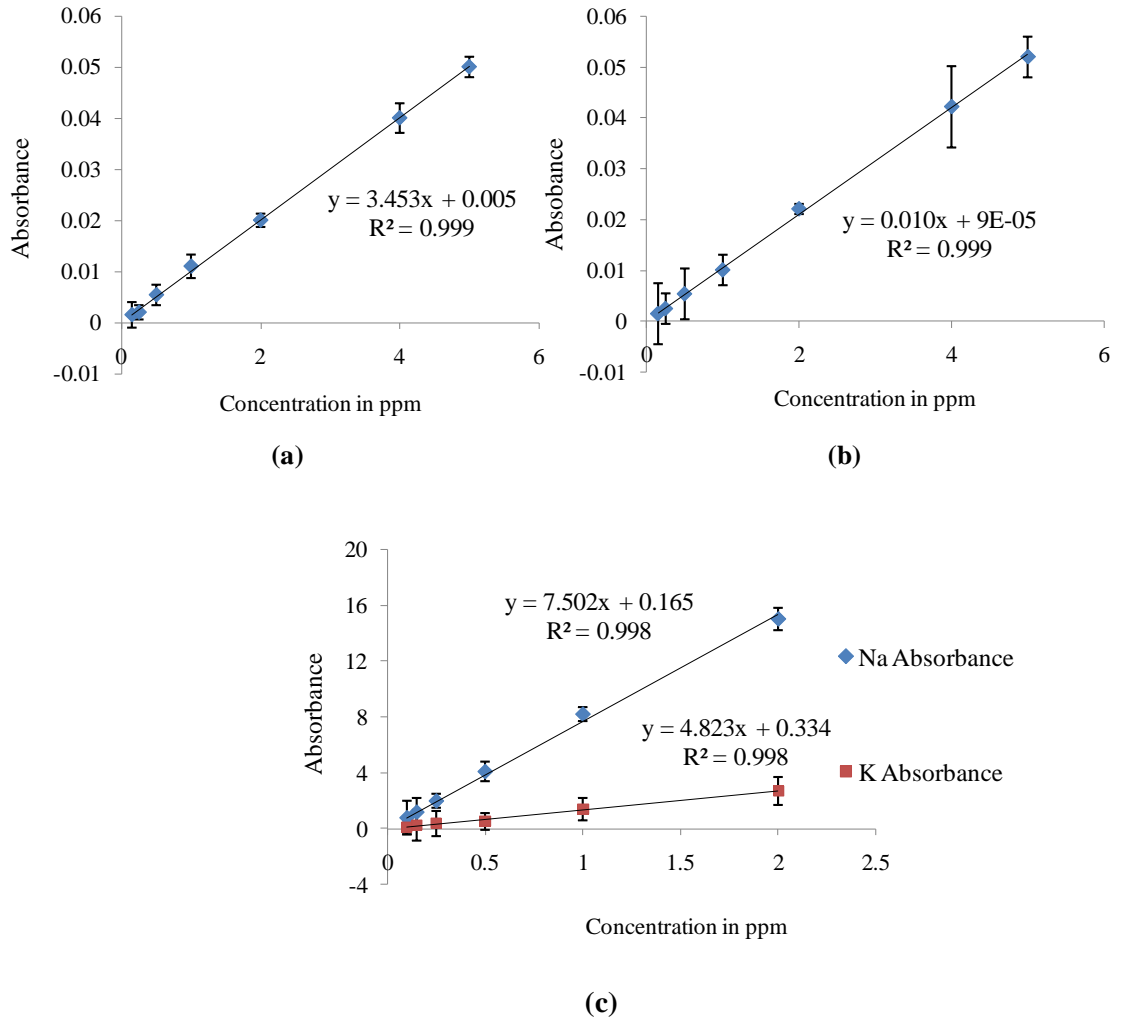


Figure 3.6: A concentration versus absorbance curve for; (a) Mg<sup>2+</sup> (b) Ca<sup>2+</sup> and (c) Na<sup>+</sup> and K<sup>+</sup>

The square of the product moment correlation coefficient ( $R^2$ ) values ranged between 0.993 for K<sup>+</sup> and 0.999 for Ca<sup>2+</sup> standards which indicated linearity of the calibration graph. The CEC of individual ions and the total thereof is indicated in (Table 3.3). In all the samples, CEC of Na<sup>+</sup> ions in the clay gallery spaces was the highest meaning that the clay exchange sites contains mostly Na<sup>+</sup> ions followed by Mg<sup>2+</sup> and K<sup>+</sup> while that of Ca<sup>2+</sup> had the lowest quantity. High CEC in soils A, C and D depended on mineralogical

composition of the soil sample. The difference in CEC values of the soils A, C and D may have been as a result of the amount of organic matter present which may have contributed to higher CEC values (table 3.3).

**Table 3.3: Total CEC of the different clays**

Cation Exchange Capacity (meq/ 100 g)					
Sample	Ca <sup>2+</sup>	Mg <sup>2+</sup>	Na <sup>+</sup>	K <sup>+</sup>	Total CEC
A	0.003	4.6817	81.2200	3.2520	89.1567 ±0.2
B	0.0003	0.7892	65.6400	1.3010	67.7332±0.4
C	0.0035	4.1033	82.5500	2.2764	88.9332±0.2
D	0.0009	5.3667	83.2120	1.6259	90.2055 ±0.1

According to Aprile and Lorinda, (2012), the most important exchangeable cations in the soil are calcium (Ca<sup>2+</sup>), magnesium (Mg<sup>2+</sup>), sodium (Na<sup>+</sup>) and potassium (K<sup>+</sup>). High CEC values of more than 75meq/100g indicates soil content with more than 80 % montmorillonite clay present (Calabria *et al.*, 2013), and this indicated that soil A, C and D was montmorillonite clay as earlier indicated by FT-IR and XRD techniques while soil B had mixtures of montmorillonite and illite clay minerals.

### 3.3 HDTMA and TMPA modified clays

Clay D was modified using HDTMA and TMPA organic cations and results are presented in the following sub-sections

#### 3.3.1 FT-IR spectra

The FT-IR spectra (Figure 3.7) after modification of clay, indicated presence of intercalated HDTMA<sup>+</sup> (appendix 15), as extra intense peaks at 2929.7 cm<sup>-1</sup> and 2856.4 cm<sup>-1</sup> attributed to the CH<sub>2</sub> anti-symmetrical stretching vibrations and CH<sub>2</sub> symmetrical vibrations respectively that had been observed in the pure HDTMA-Br.

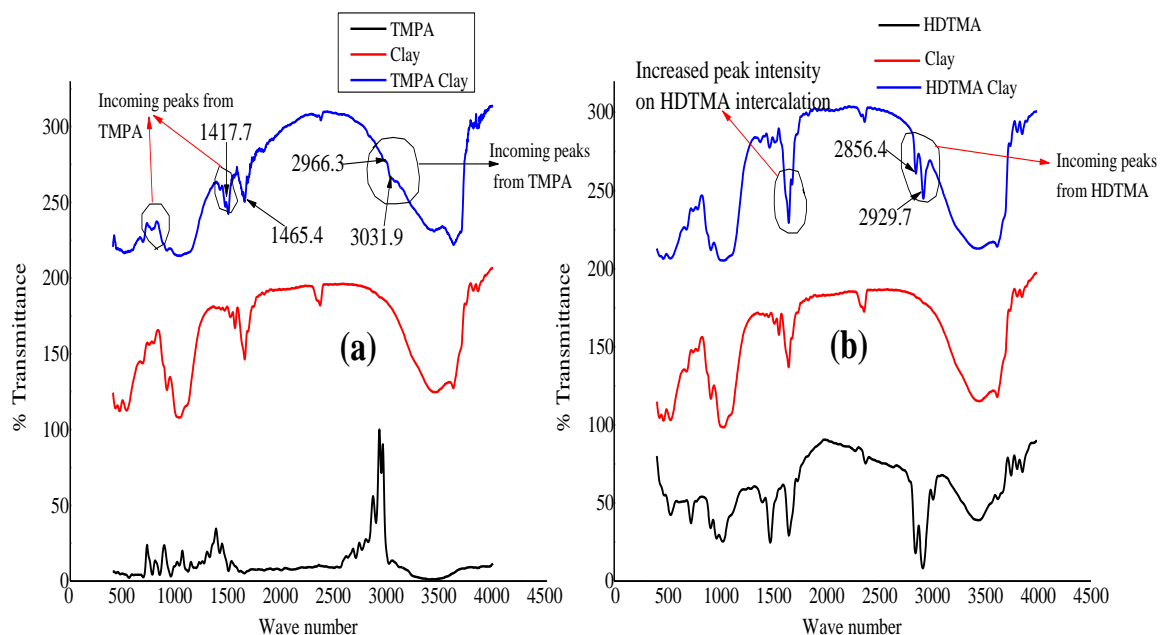


**Figure 3.7: FT-IR spectra for clay (a) modified with TMPA and (b) modified with HDTMA**

This confirmed presence of intercalated HDTMA<sup>+</sup> in the montmorillonite clay. On modification of clays with TMPA (appendix 15), peaks at 1417.6 cm<sup>-1</sup> and 1465.8 cm<sup>-1</sup> were observed ascribed to the phenyl ring of the TMPA cation confirming intercalation. The new bands at 2966.3 cm<sup>-1</sup> and 3031.9 cm<sup>-1</sup> were attributed to symmetrical stretching vibration of C-CH<sub>2</sub> of alkyl chain while the band around 1487-1490cm<sup>-1</sup> was assigned to the trimethylammonium quaternary group vibration C-N(CH<sub>3</sub>)<sub>3</sub><sup>+</sup> (Aroke and El-Nafaty, 2014; Musleh *et al.*, 2014; Navratilova *et al.*, 2007; Wong *et al.*, 1997).

### 3.3.2 XRD Analysis

Upon HDTMA intercalation into the raw sample, the peaks shifted to d<sub>(001)</sub> 12.1904 Å; d<sub>(002)</sub> at 5.5056 Å; d<sub>(112)</sub> at 3.2879 Å and d<sub>(113)</sub> at 3.2283 Å which signified increment of the basal spacing as an evidence of successful intercalation (Figure 3.8).

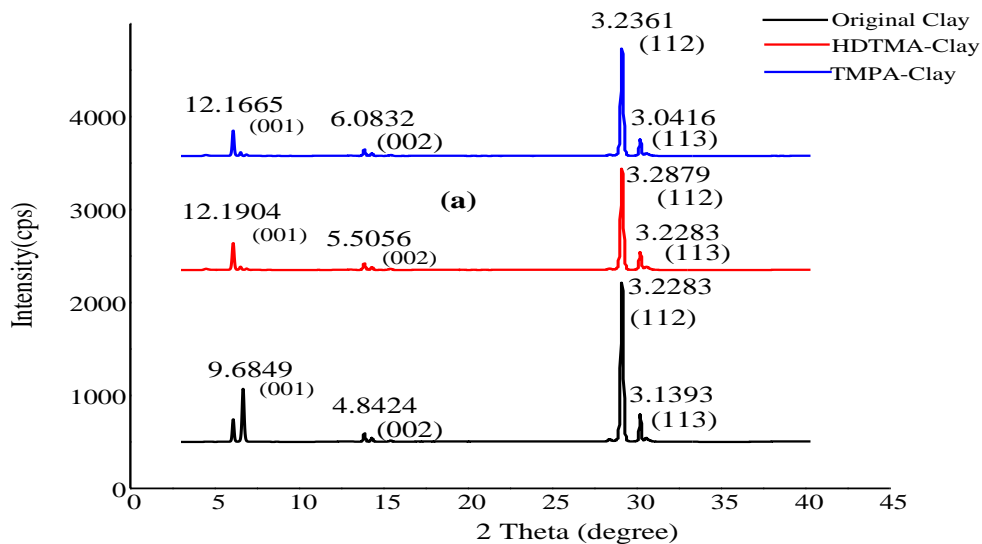


**Figure 3.8: XRD diffraction patterns for different clay materials**

Basal spacing increment on TMPA intercalation to 12.1665 Å, 6.0832 Å, 3.2361 Å and 3.0416 Å at d (001), d (002), d (112) and d (113) miller indices respectively. The observed basal spacing difference on HDTMA and TMPA modification (table 3.4), can be explained by the fact that TMPA and HDTMA are short chain and long chain alkyl ammonium cations respectively; both may have formed mono-layer coverage. According to Zhu *et al.*, (2007), the organic cation arrangement into the clay gallery spaces may be lateral monolayer (1.45-1.47 nm), lateral bi-layer (1.75-1.85 nm) and tri-layer (1.91-2.0 nm). Similar observations were made by (Navratilova *et al.*, 2007).

**Table 3.4: Basal spacing increment on organic cations intercalation in clay**

Raw Sample (Å)	HDTMA Modified (Å)	TMPA Modified (Å)	Basal Spacing Increment on HDTMA Intercalation (Å)	Basal Spacing Increment on TMPA Intercalation (Å)
9.6849 <sub>(001)</sub>	12.1904 <sub>(001)</sub>	12.1665 <sub>(001)</sub>	2.5055	2.4814
4.8424 <sub>(002)</sub>	5.5056 <sub>(002)</sub>	6.0832 <sub>(002)</sub>	0.6632	1.2408
3.2283 <sub>(112)</sub>	3.2879 <sub>(112)</sub>	3.2361 <sub>(112)</sub>	0.0596	0.0078
3.1393 <sub>(113)</sub>	3.2283 <sub>(113)</sub>	3.0416 <sub>(113)</sub>	0.089	-0.0977

### 3.4 PFE sorption kinetics

The optimal parameters for the sorption of PFE in clay materials were investigated and the results are presented in the subsequent sections.

#### 3.4.1 The effect of pH

The sorption of PFE pesticide in clay was significantly influenced by pH in the unmodified and TMPA modified clays which decreased on pH increase to 7 in the solution after 60 minutes contact time (Figure 3.9) (appendix 7 and appendix 8).

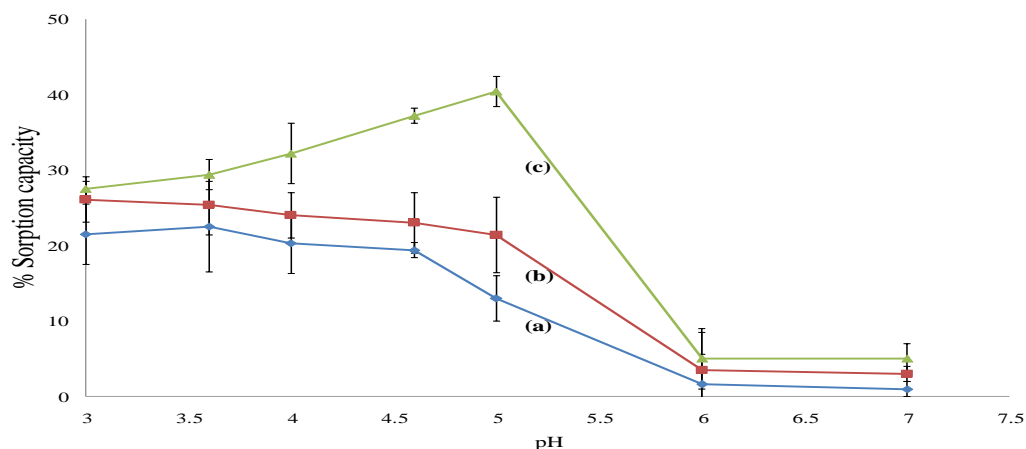


**Figure 3.9: The effect of pH on the sorption of PFE into different clay materials; (a) un-modified (b) TMPA modified and (c) HDTMA modified clay materials**

At pH 3-5, more protons are available increasing electrostatic attraction between the negatively charged PFE molecules and positively charged clay surfaces enhancing sorption in clay, TMPA and HDTMA modified clay (curves a, b and c respectively). At higher pH 7, the number of positively charged sites decreases, increasing number of negatively charged sites. These results in increased repulsive forces between PFE molecules and clay sites hence reduced sorption. This observation was in accordance with reported pesticides sorption mechanisms (Anil & Swaranjit, 2013; Boivin *et al.*, 2005; Ertli *et al.*, 2004; Floreset *et al.*, 2009; Hassani *et al.*, 2015).

### 3.4.2 Effect of temperature

Temperature is an important factor which affects the sorption of pesticide molecules into clay materials (El-Ouardi *et al.*, 2013). Figure 3.10 shows PFE sorption with increased temperature from 25 °C to 65 °C (curves a, b and c).

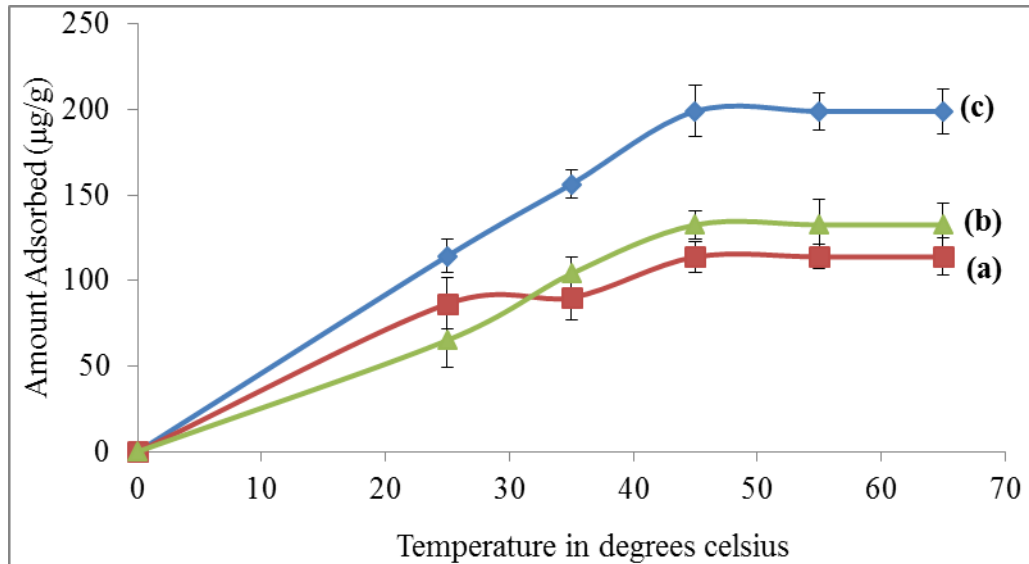


**Figure 3.10: Effect of temperature on sorption of PFE into different clay materials; (a) un-modified Clay, (b) TMPA modified clay and (c) HDTMA modified clay**

With temperature increase up to 45 °C, the PFE molecules increase in kinetic energy into the clays' gallery space resulting to increased sorption. PFE sorption into un-modified clay may be attributed to electrostatic interaction between the PFE molecules and cations present in clay gallery space, while in the modified clays may be attributed to the electrostatic interactions between the negatively charged PFE and positively charged clay gallery space. Sorption process took place to a point of saturation at (50-65 °C) (Ouzaouit *et al.*, 2013; Praus *et al.*, 2006).

### 3.4.3 Effect of initial concentration and contact time

Observations made from Figure 3.11 are that the amounts of PFE sorbed increased with time until point of saturation at 120 minutes.

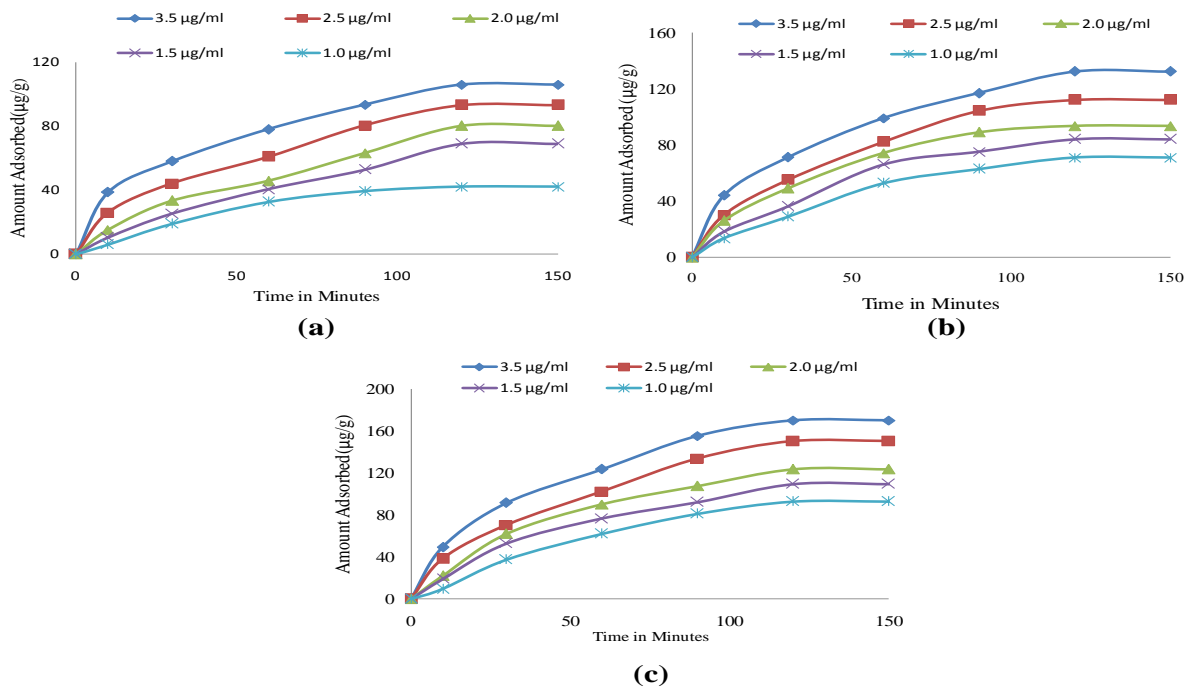


**Figure 3.11: Effect of initial concentrations at different contact time on the sorption of PFE into; (a) un-modified clay, (b) TMPA modified clay and (c) HDTMA modified clay**

The initial exponential portion in all the samples resulted due to a rapid diffusion of PFE pesticide molecules into the available sorption sites on the clay adsorbent. This was followed by linear portion which signified a gradual sorption due to low concentration of PFE molecules in the solution as well as fewer available sorption sites. This sorption process can thus be concluded to have occurred in two distinctive steps including; (i) transfer of adsorbate through external liquid film and (ii) diffusion of solute inside the adsorbent particles. Of the three samples, HDTMA modified clay was the best in the sorption of PFE pesticide molecules (El-Ouardi *et al.*, 2013; Guibal *et al.*, 2003; Mitic-Stojanovic *et al.*, 2012).

### 3.4.4 Effect of adsorbent dose

Observations made from Figure 3.12 were that, the sorption capacity increased to 97.24 %, 75.4 % and 60.5 % for 1.0 g adsorbate dose from 28.3 %, 25.3 % and 27.8 % for 0.1

g for HDTMA modified, TMPA modified and un-modified clays respectively (appendix 8).

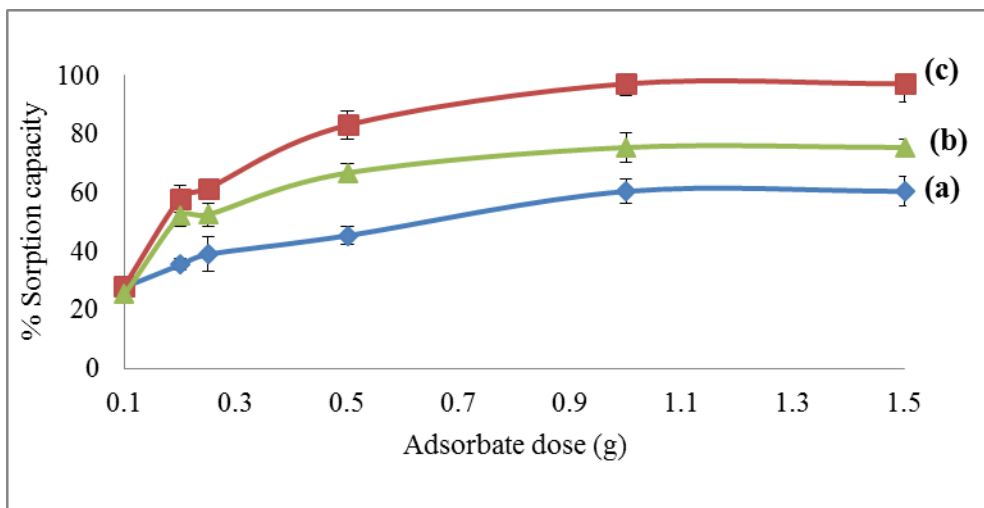


**Figure 3.12: Sorption of PFE in relation to different clay adsorbate dose; (a) Un-Modified Clay, (b) TMPA Modified Clay and (c) HDTMA Modified Clay**

Sorption capacity increased with increase in adsorbate dose due to the increased number of available sorption sites on clay surfaces to a point of saturation at 1.0 g. The HDTMA modified clay had the highest sorption efficiency which could have resulted from the modification of the clay surfaces which led to increased sorption of PFE molecules (Thavamani and Rajikumar, 2013).

### 3.4.5 Sorption isotherms

In the sorption of PFE into Un-modified clay, the data fitted best in Langmuir adsorption model as shown in Figure 3.13 (appendix 9 and appendix 10).

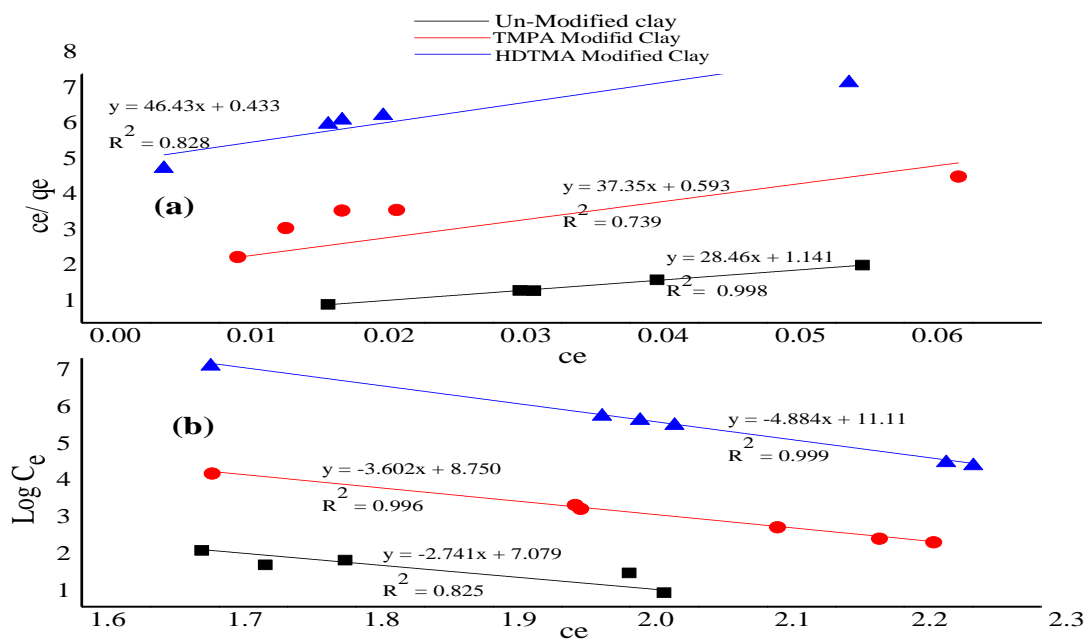


**Figure 3.13: Langmuir (a) and Freundlich (b) adsorption isotherms plots**

This was concluded from the high product moment correlation coefficient  $R^2$  of 0.998, table 3.5.

**Table 3.5: Langmuir and Freundlich parameters**

Clay Material	Langmuir Parameters			Freundlich Parameters		
	b	$Q_{\max}(\text{mg/g})$	$R^2$	$K_f$	1/n	$R^2$
Un-Modified	0.02486	0.02837	0.998	0.0018	0.2941	0.825
TMPA Modified	0.07266	0.04309	0.739	$2.5 \times 10^{-4}$	0.2822	0.996
HDTMA Modified	0.12043	0.05214	0.828	$1.306 \times 10^{-5}$	0.2060	0.999

Sorption of PFE on the un-modified clay took place on a homogeneous site, and once PFE molecules occupied a site, no further sorption took place attributed to absence of organic cations. Low  $Q_{\max}$  and b values suggested low affinity of the pesticide

molecules on the adsorbent.  $Q_{\max}$  is related to maximum sorption capacity while  $b$  is related to sorption energy. The  $Q_{\max}$  values were  $0.02837 \pm 0.0001 \text{ mg/g}$ ,  $0.05214 \pm 0.0013 \text{ mg/g}$  and  $0.04309 \pm 0.0003 \text{ mg/g}$  for un-modified, HDTMA and TMPA modified clays respectively indicating that HDTMA modified clay had the highest adsorption capacity. Similar results were observed by (Djebbar *et al.*, 2012; El-Ouardi *et al.*, 2013 and Patil and Shrivastava, 2010).

According to Gulen *et al.*, (2013); Patil & Shrivastava, (2010), separation factors  $b > 1$  signifies un-favorable sorption,  $b < 1$  signifies favorable sorption,  $b = 1$  signifies sorption process is linear while  $b = 0$  signifies that the sorption process is irreversible. With this in mind, therefore, the sorption process of PFE in the un-modified clay was best described by Langmuir isotherm as the system had homogeneous sites. Sorption involved electrophilic interactions between the PFE molecules and cations ( $\text{Ca}^{2+}$ ,  $\text{Mg}^{2+}$ ,  $\text{K}^+$ ,  $\text{Na}^+$ ) in the clay gallery spaces. Sorption of PFE in both HDTMA and TMPA modified clays was best described by Freundlich adsorption isotherm (Figure 3.13) as the correlation coefficients were in the range of  $0.97 \leq R^2 \leq 0.99$  with valid sorption of adsorbent-adsorbate system concluded from  $\frac{1}{n}$  between 0 and 1 which indicates favorable sorption.

Of the three samples, HDTMA modified clay had the lowest  $\frac{1}{n}$  value of 0.2060 indicating more favorable sorption of PFE molecules. The fact that clay surfaces are hydrophilic and on modifications with these organic cations the surfaces become hydrophobic, results to effective sorption of hydrophobic PFE molecules. Of the three samples, HDTMA modified may be the best adsorbent for the PFE pesticide molecules. This further shows the necessity of modification of clay surfaces for the sorption of pesticide molecules as observed by many researchers (Celis *et al.*, 2010; El-Ouardi *et al.*, 2013).

#### **3.4.6 Kinetic sorption models**

High correlation coefficient values, (Table 3.6), suggested that the sorption of PFE into clay materials fitted well in pseudo-second order model better than pseudo-first order

(Figure 3.14 and 3.15) at all the concentrations levels tested (appendix 11 and appendix 12).

**Table 3.6: Pseudo-first and pseudo-second order reaction kinetics for the sorption of PFE on the un-modified, TMPA modified and HDTMA modified clays**

Clay	Initial NFE Conc ( $\mu\text{g/mL}$ )	$C_e$ (Equilibrium) ( $\mu\text{g/g}$ )	Pseudo First-order Reaction Kinetics			Pseudo Second Order Reaction Kinetics		
			$R^2$	$K_1$ (1/min)	$Q_e$ (Calculated) ( $\mu\text{g/g}$ )	$R^2$	$K_2$ (g/mg min)	$Q_e$ (Calculated) ( $\mu\text{g/g}$ )
Un-Modified	1.0	0.040	0.882	$2.9 \times 10^{-3}$	0.0621	0.941	0.5745	0.0425
	1.5	0.064	0.881	$4.52 \times 10^{-3}$	0.0994	0.957	1.4312	0.0692
	2.0	0.0841	0.907	$6.72 \times 10^{-3}$	0.0292	0.924	1.1790	0.0828
	2.5	0.0932	0.785	$8.51 \times 10^{-3}$	0.0741	0.938	3.0398	0.0935
	3.5	0.1071	0.664	$9.56 \times 10^{-3}$	0.0692	0.966	7.0890	0.1052
TMPA Modified	1.0	0.0711	0.899	$2.48 \times 10^{-3}$	0.0893	0.993	7.3780	0.0741
	1.5	0.084	0.886	$2.56 \times 10^{-3}$	0.0901	0.982	1.6703	0.0841
	2.0	0.0941	0.887	$2.84 \times 10^{-3}$	0.0912	0.984	6.9178	0.0922
	2.5	0.0932	0.821	$3.22 \times 10^{-3}$	0.1364	0.973	1.3142	0.1108
HDTMA Modified	1.0	0.0930	0.892	$3.11 \times 10^{-3}$	0.0721	0.999	7.7091	0.0932
	1.5	0.1092	0.901	$2.64 \times 10^{-3}$	0.0922	0.997	6.9000	0.1094
	2.0	0.1232	0.926	$2.47 \times 10^{-3}$	0.1042	0.995	1.482	0.1206
	2.5	0.1304	0.931	$2.96 \times 10^{-3}$	0.1240	0.995	1.7236	0.1546
	3.5	0.1702	0.826	$2.50 \times 10^{-3}$	0.1511	0.995	1.4592	0.1706

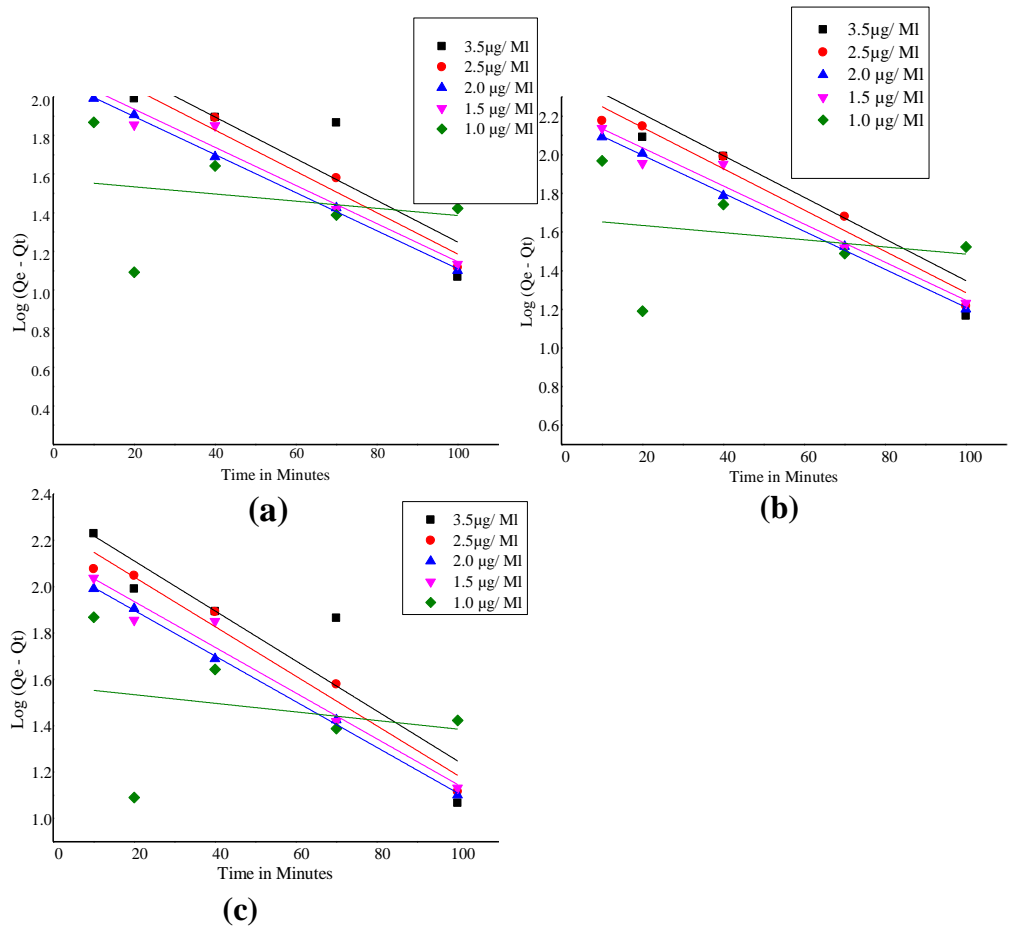


**Figure 3.14: Pseudo first order kinetics model for the sorption of PFE into (a) unmodified clay, (b) TMPA modified clay and (c) HDTMA modified clay**

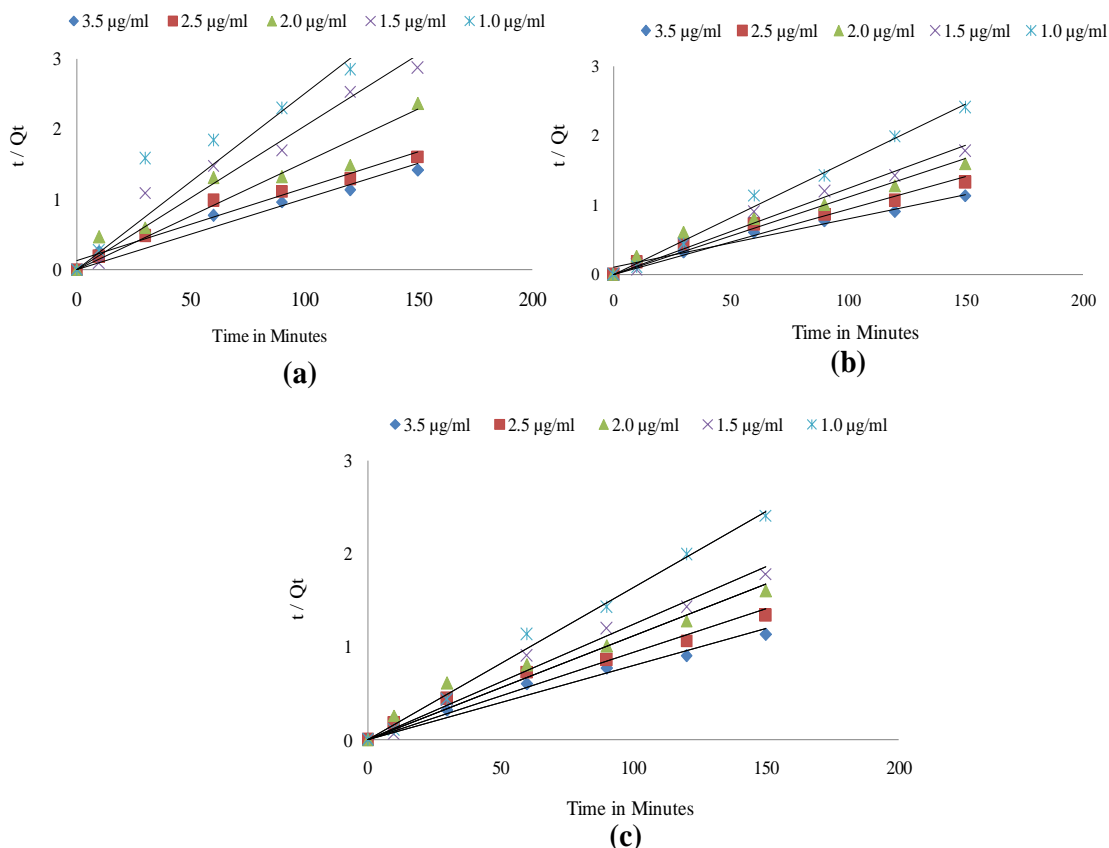


**Figure 3.15: Pseudo second order kinetics model for the sorption of PFE into; (a) un-modified clay, (b) TMPA modified clay and (c) HDTMA modified clay at different concentrations**

Moreover, the  $Q_e$  estimated by pseudo-second order model (Table 4.7) gave closer values to those of experimental  $Q_e$  values in comparison with pseudo-first order model. According to pseudo second order kinetics principle, this suggested that the rate limiting step may have been sorption on a heterogeneous/ multiple surfaces; clay and organo-clay surface, through exchange of electrons between the positively charged organic cations and negatively charged PFE molecules. Moreover, the sorption involved electrophilic interactions between the PFE molecules and cations ( $\text{Ca}^{2+}$ ,  $\text{Mg}^{2+}$ ,  $\text{K}^+$ ,  $\text{Na}^+$ ) in the clay gallery spaces (Veli and Alyuz, 2007).

### 3.5 Intercalation of PFE in clay materials

There was successful intercalation of pyrethrins as there was enhancement in peak intensities attributed to overlapping of the functional groups from PFE and the clay materials (Figure 3.16).

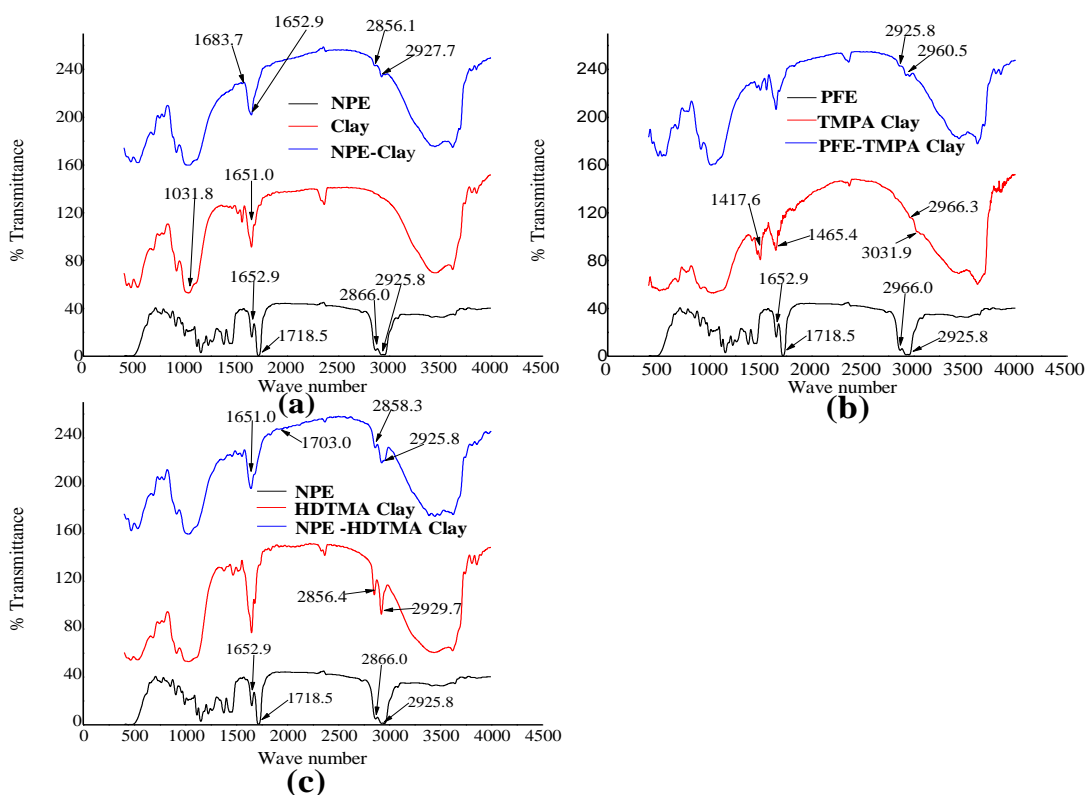


**Figure 3:16: FT-IR spectra of; (a) PFE intercalated in un-modified clay; (b) PFE in TMPA modified clay and (c) PFE in HDTMA modified clay**

Two peaks at  $2860\text{ cm}^{-1}$  and  $2925.8\text{ cm}^{-1}$  attributed to C-H asymmetrical and symmetrical of both Jasmolins and Cinerins in PFE were observed to cause shifts in the absorption bands of the clay materials. New peaks at  $2856.1\text{ cm}^{-1}$  and  $2927.7\text{ cm}^{-1}$  were observed on PFE-clay, reduced peak intensity was observed in PFE-TMPA clay shifting from  $2966.3\text{ cm}^{-1}$  and  $3031.9\text{ cm}^{-1}$  to  $2925.8\text{ cm}^{-1}$  and  $2960.5\text{ cm}^{-1}$  and on PFE-HDTMA

clay shift from 2856.4 cm<sup>-1</sup> and 2927.7 cm<sup>-1</sup> to 2858.3 cm<sup>-1</sup> and 2925.8 cm<sup>-1</sup> respectively (Essig and Zhao, 2001). Intercalation of pyrethrins in clay gallery spaces was confirmed by the increase in the basal spacing (table 3.7) of the main un-modified and organo-clay peaks(Figure 3.17).

**Table 3.7: Basal spacing variations on PFE intercalation in clay gallery spaces**

Original sample Å	<u>Increase in basal spacing on pyrethrins intercalation</u>		
	Un-modified clay	TMPA clay	HDTMA clay
9.6849	1.4434	2.8096	0.1059
4.8424	0.7217	1.9944	0.0530
3.2283	-0.0012	0.0528	0.1277
3.1393	-0.0043	0.0110	0.0977

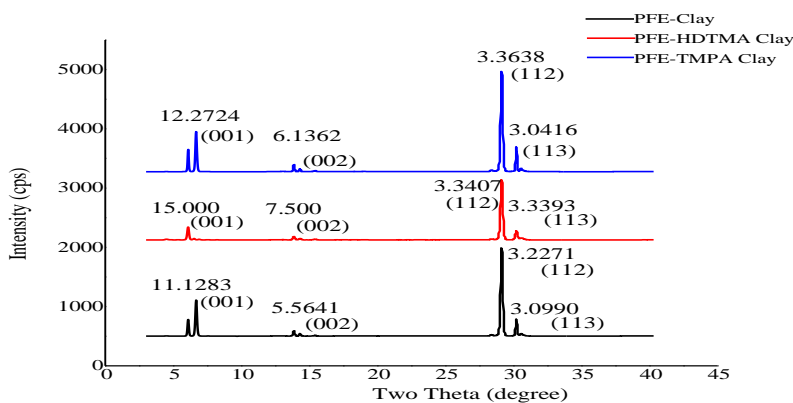


**Figure 3:17: The XRD patterns of PFE intercalated in different clay materials**

All the clay samples; the un-modified and modified sorbed pyrethrins; however, HDTMA-clay composite was more efficient. This could have resulted from increased electrostatic attraction between electrophilic HDTMA cations (long chain cation) covering the whole interlayer surface and nucleophilic pyrethrins molecules in

comparison with TMPA organo-clay. The sorbed pyrethrins pesticide molecules may have formed monolayer coverage on all the clay materials. The decrease in peak intensity also signified intercalation of the molecules. Similar results were found in case of benzene and pyridinium rings (have related structures) attaching into clay interlayer spaces(Navratilova *et al.*, 2007; Praus *et al.*, 2006).

### 3.6 Accelerated stability test

Calibration curve for pyrethrins standards was plotted and the unknown concentrations of PFE in the clay samples determined by interpolation(Figure 3.18).

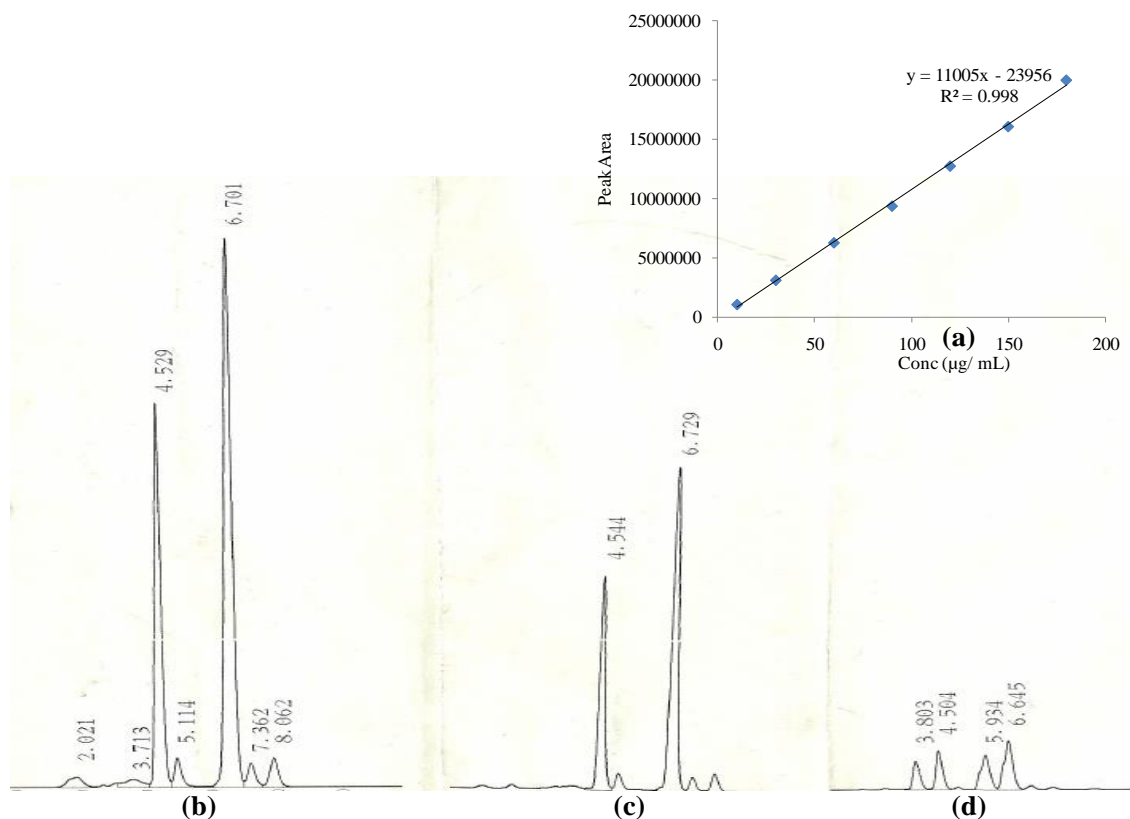


**Figure 3:18: (a) A HPLC chromatogram for (a) concentration versus peak area calibration curve for PFE together with (b) pyrethrins standard, (c) pyrethrins at HDTMA modified clay after 4 hours natural sunlight exposure and (d) control PFE after 4 hours natural sunlight**

Natural sunlight caused the highest degradation of the PFE molecules compared with the artificial UV radiations; this may be ascribed to the influence of other environmental factors like moisture, oxygen and temperature (Atkinson *et al.*, 2004). Other losses could have been as a result of evaporation rather than photo-degradation of these pyrethrins. HDTMA modified clay had the best photo-stabilization effect. About 63.4 % and 11.13 % pyrethrins in PFE-HDTMA clay and unprotected PFE (control) respectively were undecomposed on exposure to sunlight (Figure3.19) (appendix 13).

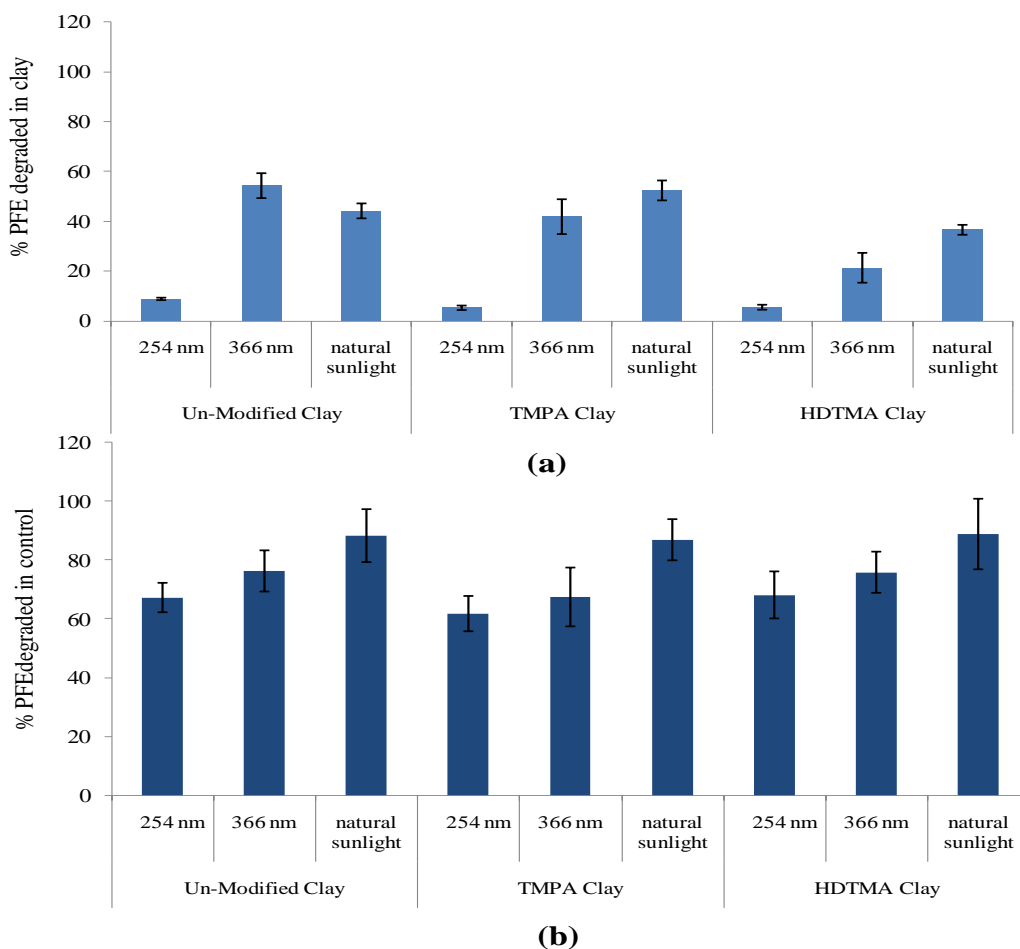


**Figure 3:19: Protective effect of different clay materials on PFE pesticide; (a) PFE in clay and (b) control PFE**

This may have been as a result of more PFE intercalation in the gallery space and consequently more protection against direct UV light and active oxygen species

degradation. Moreover, the cationic organic chromophores; HDTMA and TMPA intercalated in clay materials may have acted as energy/charge acceptor to the photo-excited PFE pesticide molecule, which returned to its ground state and became photo-stabilized or may have absorbed light and prevented photo-excitation of the PFE pesticide molecules and this lengthened its degradation lifetime. Steric hindrance of the cations and the PFE pesticide from the radiations may also have reduced the photochemical degradation process. This further proved the necessity of modifying the clay materials for pesticide sorption (Celiset *et al.*, 2010; El-Nahhal *et al.*, (2001).

### **3.6.1 Photo-degradation of pyrethrins**

Pyrethrins pesticides are highly degraded by sunlight after they are exposed into the environment. The extent of sunlight photolysis is highly dependent on UV absorption profile of the pesticide, surrounding medium and the emission spectrum of sunlight. The energy to break chemical bonds in pesticide molecules ranges from 70-120 kcalmol<sup>-1</sup> corresponding to 250-400nm.

When a photon from sunlight passed close to the PFEs pesticide molecule, molecular excitation occurred through the interaction between the electric field of the pesticide and that of sunlight without changing the molecular geometry. Each photon activated a molecule in ground state ( $\pi$ ) to excited state ( $\pi^*$ ) transition state due to presence of the aromatic moiety in the pyrethrins structure.

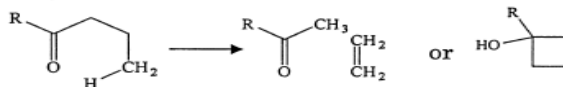
#### **3.6.1.1 The photo-chemical reaction**

The photo induced cleavage of the c-c bond generated a ketyl radical at the carbonyl carbon in the excited state abstracting hydrogen from neighboring alkyl group. The electronic transition also occurred at the aromatic moiety which resulted in cis or trans geometry isomerization. The photo induced homolytic bond occurred on ester or ketone moiety and decarboxylation or decarbonylation proceeded (Figure 3.20).

1. Norrish type-I reaction

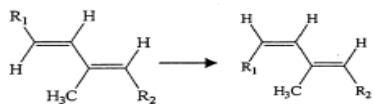


2. Norrish type-II reaction

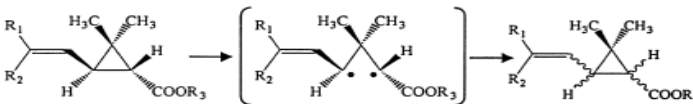


3. Isomerization (geometrical or optical)

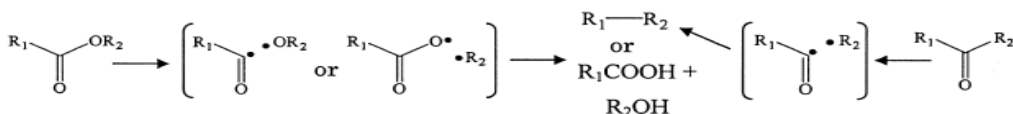
(a)



(b)



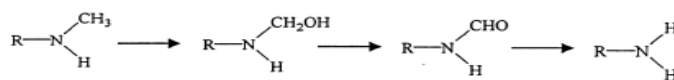
4. Ester cleavage, decarboxylation, decarbonylation



5. Dehalogenation



6. Dealkylation



7. C-Oxidation

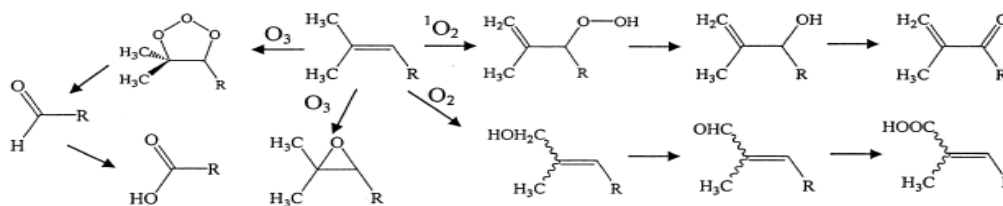


Figure 3:20: Degradation of pyrethrins by UV light (Katagi, 2004)

### 3.6.1.2 Photo protection of the clays and organo clays to PFE pesticides

Sorption of PFEs into clays and organo clays affected the photo-physical process. Molecular motion was highly restricted and PFEs interaction with these heterogeneous surfaces resulted in modification of their electronic surfaces. On sorption of PFEs onto clay materials there were spectra changes characterized by spectra shift, changes in

extinction coefficient, broadening of the absorption band and appearance of new bands. Both the bathochromic ( $\pi\text{-}\pi^*$ ) and hypsochromic ( $n\text{-}\pi^*$ ) shifts would have occurred in the PFEs. The alteration of emission spectrum of the PFEs resulted in significant increase in fluorescence intensity when sorbed into clay interlayer. The increase in intensity is likely to stem from an inhibition of radiationless quenching by counteranion  $\text{Cl}^-$  by intercalation of PFE molecules into clay interlayer.

Organo clays pyrethrins formulation was composed of pyrethrins as the active ingredient and clays as carrier materials. The organic cations have both the hydrophobic and hydrophilic parts of the molecule which provided a very complex medium for photolysis of the PFEs pesticide and their moiety became a possible photo-sensitizer or quencher.

The other possible effect of the cations was the stabilization of photo-induced radicals of PFEs in the clay interlayer space. This involved the energy transfer involving  $\pi\text{-}\pi^*$  transitions between the triplet states of the PFEs and the organic cations. Consequently, modification of clay surfaces with the organic cations may have lowered the production of these radicals and thus yielding photo stabilization effect.

On the other hand, the organic cations may not have been involved in photo protection of PFEs. Their role would have been to enhance PFEs sorption into clay materials while clay mineral may have acted as a photo protector. The steric hinderance of the clay surfaces may have been the result of photo protection of the PFEs.

### **3.7 Bioassay tests on maize weevils**

There was a significant difference ( $p = 0.05$ ) in the weevils' mortality rate due to the different clay treatments (Table 3.8).

**Table 3.8: Analysis of Variance (ANOVA) for the different carriers at different dosage rates**

<b>Within sample subject effects</b>	<b>Sum of squares</b>	<b>Mean square</b>	<b>Degree of freedom</b>	<b>Probability &gt;F</b>
<b>Dosage</b>	<b>110.4500</b>	<b>10.5095</b>	<b>1</b>	<b>0.0030</b>
<b>Time</b>	<b>778.3620</b>	<b>27.8991</b>	<b>4</b>	<b>1.2728 x 10<sup>-6</sup></b>
<b>Dosage * Time</b>	<b>39.6250</b>	<b>9.9063</b>	<b>4</b>	<b>0.0052</b>
<b>Between sample Subject effect</b>	<b>Sum of squares</b>	<b>Mean square</b>	<b>Degree of freedom</b>	<b>Probability &gt;F</b>
	<b>4207.9005</b>	<b>64.8683</b>	<b>1</b>	<b>0.01209</b>

The un-degraded PFE was the most effective closely followed by PFE-HDTMA clay at 100 % and 58 % respectively when applied at 0.5 g / 30 g maize grain after 48 hours exposure. Mortality rate increased with increased exposure time and concentration in all the different sample treatments (Figure 3.21) (appendix 14).

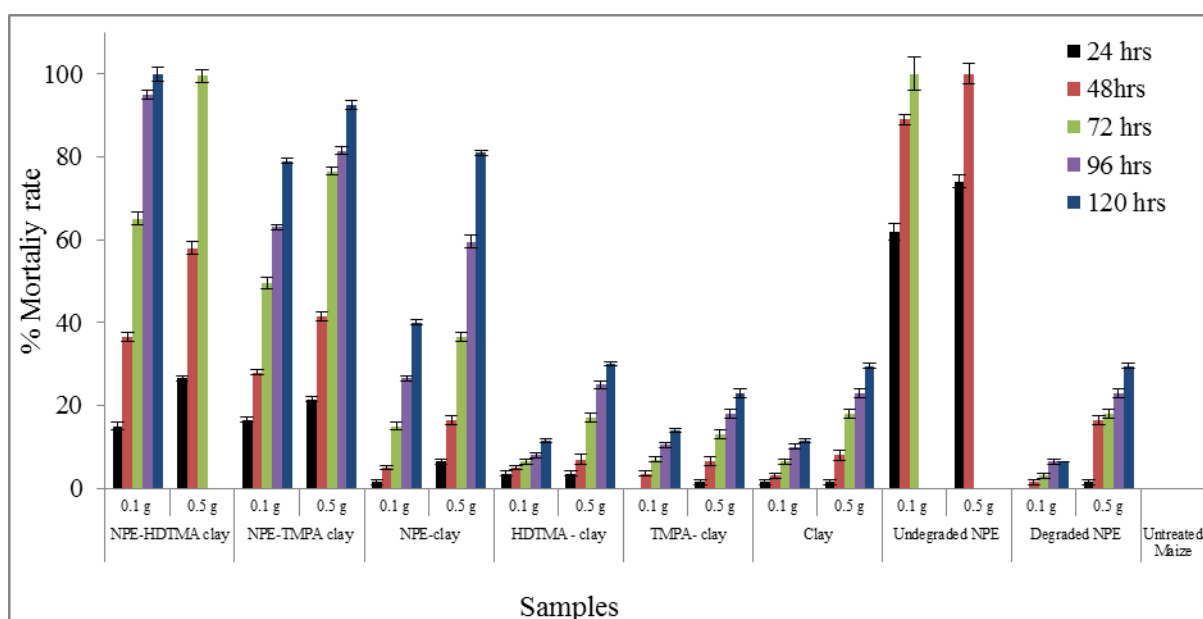


**Figure 3:21: Mortality rate (%) of maize weevils (*Sitophilus zeamais*) at different dosage rates within different carriers administered at varying times**

This may have been due to the increased contact poison for an increased period of time and consequently led to their death. Pyrethrins are contact poison that rapidly penetrated to the weevils' nervous system, block the nerve junction and the action of sodium channels causing knock-down effect, paralysis and later death (Davies *et al.*, 2007). There was a significant difference ( $p = 0.05$ ) in the mortality rate for PFE-HDTMA clay, PFE-TMPA clay and PFE-clay treatments at 48 hours exposure (Table 3.9). Similar observations of increased mortality at increased treatment concentration were made by Abdullahi *et al.*, (2014) in *Sitophilus zeamais* control using *Acacia nilotica* bark and root powders.

**Table 3.9: Cumulative means of different clay treatments on maize weevils (*Sitophilus zeamais*) mortality rate**

	Dosage (g/ 30 g grains)	24 hrs	48 hrs	72 hrs	96 hrs	120 hrs
NPE-HDTMA-Clay	0.1 g	3 ± 1 <sup>(a)</sup>	7.3 ± 1.2 <sup>(b)</sup>	13 ± 1.6 <sup>(c)</sup>	19 ± 1 <sup>(d)</sup>	20 ± 0.0 <sup>(d)</sup>
	0.5 g	5.3 ± 0.58 <sup>(a)</sup>	11.6 ± 1.6 <sup>(b)</sup>	19.9 ± 0.1 <sup>(c)</sup>	19.9 ± 0.1 <sup>(c)</sup>	19.9 ± 0.1 <sup>(c)</sup>
NPE-TMPA clay	0.1 g	3.3 ± 0.6 <sup>(a)</sup>	5.6 ± 0.6 <sup>(b)</sup>	9.9 ± 1.6 <sup>(c)</sup>	14.6 ± 0.6 <sup>(d)</sup>	19.9 ± 0.6 <sup>(e)</sup>
	0.5 g	4.3 ± 0.6 <sup>(a)</sup>	8.3 ± 1 <sup>(b)</sup>	15.3 ± 1 <sup>(c)</sup>	18.3 ± 1 <sup>(d)</sup>	19.3 ± 1 <sup>(e)</sup>
NPE-Clay	0.1 g	0.3 ± 0.6 <sup>(a)</sup>	1 ± 0.6 <sup>(a)</sup>	3 ± 1 <sup>(b)</sup>	5.3 ± 0.6 <sup>(c)</sup>	8 ± 0.6 <sup>(d)</sup>
	0.5 g	1.3 ± 0.6 <sup>(a)</sup>	3.3 ± 1 <sup>(b)</sup>	7.3 ± 1 <sup>(c)</sup>	11.9 ± 1.5 <sup>(d)</sup>	16.2 ± 0.6 <sup>(e)</sup>
HDTMA-Clay	0.1 g	0.7 ± 0.6 <sup>(a)</sup>	1 ± 0.6 <sup>(a)</sup>	1.3 ± 0.6 <sup>(a)</sup>	1.6 ± 0.6 <sup>(a)</sup>	2.3 ± 0.6 <sup>(a)</sup>
	0.5 g	0.7 ± 0.6 <sup>(a)</sup>	3.4 ± 1.2 <sup>(b)</sup>	5.4 ± 1 <sup>(c)</sup>	7.4 ± 1 <sup>(d)</sup>	9.1 ± 0.6 <sup>(e)</sup>
TMPA-Clay	0.1 g	0 ± 0.0 <sup>(a)</sup>	0.7 ± 0.6 <sup>(a)</sup>	1.4 ± 0.6 <sup>(a)</sup>	2.1 ± 0.6 <sup>(a)</sup>	2.8 ± 0.6 <sup>(a)</sup>
	0.5 g	0.3 ± 0.6 <sup>(a)</sup>	1.3 ± 1 <sup>(a)</sup>	2.6 ± 1.2 <sup>(a)</sup>	3.6 ± 1.0 <sup>(a)</sup>	4.6 ± 1.0 <sup>(a)</sup>
Clay	0.1 g	0.3 ± 0.6 <sup>(a)</sup>	0.6 ± 0.6 <sup>(a)</sup>	1.3 ± 0.6 <sup>(a)</sup>	2 ± 0.6 <sup>(a)</sup>	2.3 ± 0.6 <sup>(a)</sup>
	0.5 g	0.3 ± 0.6 <sup>(a)</sup>	1.6 ± 1.2 <sup>(a)</sup>	3.6 ± 1.0 <sup>(b)</sup>	4.6 ± 0.7 <sup>(b)</sup>	5.9 ± 0.6 <sup>(b)</sup>
Un-degraded NPE	0.1 g	12.3 ± 0.6 <sup>(a)</sup>	17.6 ± 0.6 <sup>(b)</sup>	17.6 ± 0.6 <sup>(b)</sup>	18.6 ± 0.5 <sup>(b)</sup>	19.9 ± 0.1 <sup>(b)</sup>
	0.5 g	5.3 ± 1.0 <sup>(a)</sup>	19.6 ± 2.1 <sup>(b)</sup>	19.9 ± 2.1 <sup>(b)</sup>	19.9 ± 2.1 <sup>(b)</sup>	19.9 ± 2.1 <sup>(b)</sup>
Degraded NPE	0.1 g	0 ± 0.0 <sup>(a)</sup>	0.3 ± 0.6 <sup>(a)</sup>	0.6 ± 0.6 <sup>(a)</sup>	1.3 ± 0.6 <sup>(a)</sup>	1.3 ± 0.6 <sup>(a)</sup>
	0.5 g	0.3 ± 0.6 <sup>(a)</sup>	1.6 ± 1.2 <sup>(a)</sup>	3.6 ± 1.0 <sup>(b)</sup>	4.6 ± 1.0 <sup>(b)</sup>	5.9 ± 0.6 <sup>(b)</sup>

Means with same superscripts in brackets across a row represent no significant difference at 5% probability level

Un-degraded PFE pesticide present in the clays was responsible for the death of the weevils. However, PFE present in HDTMA clay was in higher quantities in comparison to both TMPA clay and Un-modified clay even after 4hours of exposure to sunlight before the experiment kicked off (photo stabilization) and consequently resulted to highest mortality rate.

There was no significant difference at ( $p = 0.05$ ) among HDTMA clay, TMPA clay and Clay in weevils' mortality rate and only caused deaths in the range of 1-30 %. This further proved that the cations added to clay had no effect on the weevils' death and only acted as agent that increased the PFE sorption into clay. However, according to Masiwa (2004), the clays have the capacity to absorb massive water and causing dehydration to the weevils leading to their death. High clay concentrations resulted in higher chances of the weevils 'dust pick up and consequently desiccation of the insects (Figure 3.20). Degraded PFE had the lowest maize weevils' mortality rate due to its unprotected state from the UV light. According to Antonious, (2004), pyrethrins degrade from 100 - 1 % on exposure to field conditions within 5 hours. Combination of two effective samples; clay and PFE proved to have the best results in maize weevils' eradication and farmers should embrace this technology. As expected, there was no mortality in the control as there was no maize protection.

Clay is extremely stable leaving no chemical residues on the treated produce thus has no health problem to the final consumer. Moreover, winnowing, a physical process removes about 98% of this dust from the treated grains. Pyrethrins on the other hand, can be used against a wide range of pests and breaks down easily, leaving no residues to the maize grains and consequently no chemical toxicity to the final consumer (Kariuki *et al.*, 2014).

## CHAPTER FOUR

### CONCLUSION AND RECOMMENDATIONS

#### 4.1 CONCLUSIONS

The naturally occurring clay mineral was characterized to be MMT clay as confirmed by XRF, FT-IR and XRD characterization techniques. The clay spectrum obtained from the FT-IR technique indicated presence of MMT clay mineral further confirming the XRF results. According to the XRD diffraction clay patterns MMT clay mineral had the highest quantity in comparison to the other minerals present in clay. Sorption isotherms confirmed that HDTMA-clay to be the best pyrethrins sorbent and sorption occurred on a heterogeneous surface. Pyrethrins were photo-stabilized with MMT-clay showing a marked increase in its photo-protection. HDTMA-Clay had the highest photo-stabilizing effect in comparison with other clay materials. Bioassay study showed that PFE-HDTMA clay can be a potential maize grain protectant against maize weevils (*Sitophilus zeamais*) due to considerable mortality rates at low dosage. Clay samples also had subsequent amounts of the mortality rates due to their desiccant property. This therefore requires sourcing for this local, environmental friendly, economical, most precious clay mineral for use as PFE pesticide carrier. Clay is very stable and winnowing the food products (cereals) would assist in removing the dust. Pyrethrins on the other hand, can be used against a wide range of pests and breaks down easily, leaves no residues to the food materials. Combination of the two materials resulted to a spectacular pesticide formulation in control of maize weevils. Successful photo-stabilization of the pyrethrins pesticide based formulation will improve the marketability of the pyrethrum flowers, improve economic utilization of clay deposits and consequently boost food security in Kenya and globally at large. Kenyan farmers strive to have maximum maize protection at low pesticide doses and PFE-HDTMA clay proved to be more efficient at low dosage.

## **4.2RECOMMENDATIONS**

### **4.2.1 Recommendations from this work**

1. Wider research on the photo-protection behavior of MMT on pyrethrins modified with intercalation of other cations.
2. More research should be geared towards investigation of organo-MMT pyrethrins composites on its effectiveness in control of a wide range of pests on horticultural crops in the field.

### **4.2.2 Recommendations for further work**

1. Cheaper and greener synthesis of pyrethrins photo-protectors techniques needs to be explored in order to come up with viable systems which would compete with conventional pyrethrins photo-protectors ( Ononye, Mogbo and Akunne 2013).

## REFERENCES

- Abdullahi, N., Umar, Z. & Babura, S. (2014). Comparative efficacy of the bark and root powders of *Acacia nilotica* against maize weevil *Sitophilus zeamais* (Motschulsky) (Coleoptera: Curculionidae) in Kano state of Nigeria. *African Journal of Agriculture Research*, 9, 588-92.
- Adikary, S.U. and Wanasinghe, D.D. (2012). *Characterization of locally available montmorillonite clay using FTIR technique*, PhD Thesis, Hong Kong: University of Moratuwa,
- Akunne, C. E., Ononye, B.U. & Mogbo, T.C. (2013). Evaluation of efficacy of mixed leaf powder of *Vernonia amygdalina*(L.) and *Azadirachta indica* (A. Juss) against *Callosobruchus macalatus*(F.) (Coleoptera: Bruchidae). *Advances in Bioscienceand Bioengineering*, 1, 86-89.
- Anil, K. & Swaranjit, S. (2013). Adsorption and desorption behavior of chlorotriazine herbicide in the agriculture soils. *Journal of Petroleum and Environmental Biotechnology*, 4, 154-155.
- Antoaneta, E., Alina, B. & Georgescu, L. (2009). Determination of heavy metals in soils using XRF technique. *Journal of Romanian Reports of Physics*, 55, 815-820.
- Antonious, G. (2004). Residues and half-life of pyrethrins on field-grown pepper and tomato. *Journal of Environmental Science and Health*, 39, 491-503.
- Aprile, F. and Lorandi, R. (2012). Evaluation of cation exchange capacity (CEC) in tropical soils using for different analytical methods. *Journal of Agricultural Scienceandian center of science and education*, 150, 278-289.
- Aroke, U. & El-Nafaty, U. (2014). XRF, XRD and FTIR properties and characterization of HDTMA-Br surface modified organo-kaolinite clay. *International Journal of Emerging Technology and Advanced Engineering*, 4, 817-825.
- Arke, U. O., El-Nafaty, U. A. and Osha, O. A. (2008). Removal of oxyanion contaminants from waste water by sorption onto HDTMA-Br surface modified organo-kaolinite clay. *International Journal of Emerging Technology and Advanced Engineering*, 4, 475-484.

- Asawalam, E., Emosairue, S., Ekeleme, F. and Wokacha, R. (2006). Insecticidal effects of powdered parts of eight Nigerian plant species against maize weevils *Sitophilus zeamais* Motschulsky (Coleoptera: Curculionidae). *International Journal of Plant, Animal and Environmental Science*, 1, 106-113.
- Atkinson, B. L., Blackman, A.J. and Faber, H. (2004). The degradation of the natural pyrethrins in crop storage. *Journal of Agriculture and Food Chemistry*, 52, 280-287.
- Belmain, S., Neal, G., Ray, D. and Golob, P. (2001). Insecticidal and vertebrate toxicity associated with ethanol botanicals used as post-harvest protectants in Ghana. *Journal of Food Chemistry Toxicity*, 39, 287-291
- Bindu, P. and Thomas, S. (2014). Estimation of lattice strain in ZnO nanoparticles: X-ray peak profile analysis. *Journal of Theoretical and Applied Physics*, 8, 123-134.
- Blankson, W., Gitau, G., Stevenson, W., Philip, C. (2014). Cost: benefit analysis of botanical insecticide use in cabbage: implications for smallholder farmers in developing countries. *Journal of Crop Protection*, 57, 71-76
- Boivin, A., Cherrier, R. and Schiavon, M. (2005). A comparison of five pesticides adsorption and desorption processes in the thirteen contrasting field soils. *Journal of Chemosphere*, 61, 668-676.
- Calabria, A., Amaral, N., Ladeira, Q., Cota, S. and Silva, S. (2013). Determination of the cation exchange capacity of the bentonite exposed to the hyperalkaline fluid. *International Nuclear Atlantic Conference - INAC 2013 Recife, PE, Brazil, November 24-29, 2013 ASSOCIAÇÃO BRASILEIRA DE ENERGIA NUCLEAR - ABEN*
- Celis, R., Facenda, G., Hermosin, C. and Cornejo, J. (2007). Assessing factors influencing the release of hexazinone from clay-formulations. *International Journal of Environmental Analytical Chemistry*, 85, 1153-1164.
- Celis, R., Hermosin, C., Cornejo, L., Carrizosa, J. and Cornejo, J. (2010). Clay – herbicide complexes to retard picloram leaching in soil. *International Journal of Environmental and Analytical Chemistry*, 82, 8-9.

- Cuhna, T., Novotny, E., Madari, B., Martin-Neto, L., Rezende, L., Canelas, L. & Benites, V. (2009). Spectroscopy characterization of humic acids isolated from Amazonian Dark Earth soils. *Springer Science*, 5,363-372.
- Dafalla, M. & Ali, E. (1991). Quantitative identification of montmorillonite in clay using x-ray diffraction. *Journal of Austrarian Geomechanics*, 1, 32-34.
- Davies, T., Field, L., Usherwood, P., Williamson, M. (2007). DDT, pyrethrins, pyrethroids and insect sodium channels. *Journal of IUBMB Life*, 59, 151-162.
- Dessalgne, H., Mekonnen, A. & Indris, A. (2011). Variability of pyrethrum (*Chrysanthemum cinerariaefolium*) clones for chemical traits at Bekoji and Meraro of south eastern Ethiopia. *International Journal of Medical Aromatic Plants*, 1, 166-174.
- Djebbar, M., Djafri, F., Bouchekara, M. & Djafri, A. (2012). Adsorption of phenol on natural clay. *Journal of Applied Water Science*, 2, 77-86.
- El Ouardi, M., Alahiane, S., Qourzal, S., Abamrane, A., Assabbane, A. & Douch, J. (2013). Removal of carbaryl pesticide from aqueous solution by adsorption of local clay in Agadir. *American Journal of Analytical Chemistry*, 4, 72-79.
- El-Messabeb-Ouali, A., Benna-Zayani, M., Ayadi-Trabelsi, M., Sauvé, M., & Sauve, S. (2013). Morphology, structure, thermal stability, XR-Diffraction and infrared study of hexadecyltrimethylammonium bromide-modified smectite. *International Journal of Chemistry*, 5, 12-28.
- El-Nahhal, Y., Undabeytia, T., Polubesova, T., Mishael, G., Nir, S. & Rubin, B. (2001). Organo-clay formulation of pesticides: reduced leaching and photo-degradation. *Journal of Applied Clay Science*, 18, 309-326.
- Ertli, T., Marton, A., & Foldenyi, R. (2004). Effect of pH and the role of organic matter in the adsorption of isoproturon on soils. *Journal of Chemosphere*, 57, 771-779.
- Essig, K. & Zhao, J. (2001). Preparation and characterization of pyrethrum extracts standards. *Journal of Environmental Science*, 19,10-15.

- Eyheraguibel, B., Richard, C., Ledoigt, G. & Ter Halle, A. (2010). Photo-protection by plant extracts: A new ecological means to reduce pesticide photo-degradation. *Journal of Agriculture and Food Chemistry*, 58, 9692-9696.
- Fernandez-Perez, M., Flores-Cespedes, F., Daza-Fernandez, I., Vidal-Pena, F. & Villafranca-Sanchez, M. (2014). Lignin and lignosulfonate-based formulations to protect pyrethrins against degradation and volatilization. *Journal of Industrial and Engineering Chemistry Research*, 53, 13557-13564.
- Flores, C., Morgante, V., Gonzalez, M., Navia, R., Seeger, M. (2009). Adsorption studies of the herbicide simazine in agricultural soils of the Aconcagua valley, central Chile. *Journal of Chemosphere*, 74, 1544-1549.
- Gaber A., Abdel-Rahim, A., Abdel-Latif, Y. & Abdel-Salam, N. (2013). Influence of calcinations temperature on the structure and porosity of nanocrystalline SnO<sub>2</sub> synthesized by conventional precipitation method. *International Journal of Electrochemical Science*, 9, 81-95.
- Gadzirayi, C., Mutandwa, E. & Chikuvire, T. (2006). Effectiveness of maize cob powder in controlling weevils in stored maize grain. *Journal of African Studies Quarterly*, 8, 4-5.
- Gamiz, B., Celis, R., Hermosin, M. & Cornejo, J. (2010). Organo clays as soil amendments to increase efficacy and reduce environmental impact of the herbicide floumeton in agricultural soil. *Journal of Agriculture and Food Chemistry*, 58, 7893-7901.
- GeoEnvironmental Research Group Laboratory Manual (2008).
- Government of Kenya (2013). The Pyrethrum Act, 2013, Special Issue. Government of the Republic of Kenya Printer, Nairobi <http://kenyalaw.org/kl/fileadmin/pdfdownloads/Acts/PyrethrumActNo2of2013.PDF>. Accessed 18 Feb 2014.
- Guegan, R., Gautier, M., Beny, J. & Muller, F. (2009). Adsorption of a C10E3 non-ionic surfactant on a Ca-Smectite. *Clay and clay minerals*, 57, 502-509.

- Guibal, E., McCarrick, P. & Tobin, J. (2003). Comparison of the sorption of anionic dyes on activated carbon and chitosan derivatives from dilute solutions. *Journal of Separation Science and Technology*, 38, 3049-3073.
- Gulen, J., Altin, Z. & Ozgur, M. (2013). Adsorption of amitraz on the clay. *American Journal of Engineering Research*, 2, 1-8.
- Gupta, A., Amitabh, V., Kumari, B., & Mishra, B. (2013). FTIR and XRPD studies for the mineralogical composition of Jharkhand bentonite. *Research Journal of Pharmaceutical, Biological and Chemical Sciences*, 4, 360-369
- Hasmukh, A., Rajesh, S., Hari, C. & Raksh, V. (2006). Nano-clays for polymer nanocomposites, paints, inks, greases and cosmetics formulations, drug delivery vehicle and waste water treatment. *Journal of Bulletin of Material Science*, 29, 133-145.
- Hassani, A., Khataee, A., Karaca, S. & Shirzad-Siboni, M. (2015). Surfactant-modified montmorillonite as a nanosized adsorbent for removal of an insecticide, Kinetic and isotherm studies. *Journal of Environmental Technology*, 10, 1-42.
- Housset, P. & Dickmann, R. (2009). A promise fulfilled- pyrethroid development and benefits for agriculture and human health. *Journal of Bayer Crop Science*, 62, 135-144.
- Ileke, K. & Oni, M. (2011). Toxicity of some plant powders to maize weevil, *Sitophilus zeamais* (motschulsky)[Coleoptera: Curculionidae] on stored wheat grains(*Triticum aestivum*). *African Journal of Agricultural Research*, 6, 3043-3048.
- Ismadji, S., Soetaredjo, F. & Ayucitra, A. (2015). Natural clay minerals as environmental cleaning agents. *Journal of Clay Materials for Environmental Remediation*, 8, 5-37.
- Isman, B. (2008). Perspective botanical insecticide, for richer, for poorer. *Journal of Pest Management Science*, 64, 8-11.
- Issa, U., Afun, J., Mochiah, M., Owusu-Akyaw, M. & Haruna, B. (2001). Effect of some local botanical materials for the suppression of weevil populations.

- International Journal of Plant, Animal and Environmental Sciences*, 1, 2231-4490.
- James, O., Mesubi, M.A., Adekola, F.A., Odebunmi, E.O., & Adekeye, J.A. (2008). Beneficiation and characterization of a bentonite from north-eastern Nigerian. *Journal of the North Carolina Academy of Science*, 124, 154-158.
- Jana, D. (2007). Pyrethrum (*Tanacetum Cinerariifolium*) from northern Adriatic as a potential source of natural insecticide. *Original Scientific Journal*, 17, 39-46.
- Kariuki, D., Njiru, S., Miaron, J. Kariuki, D. & Mugweru, J. (2014). Synergistic bio-pesticide combination of pyrethrins and rotenoids for the control of the cockroach *Americana Periplaneta*. *International Journal of Humanities, Arts*, 2, 43-48.
- Kasaj, D., Rieder, A., Krenn, L. & Kopp, B. (1999). Separation and quantitative analysis of natural pyrethrins by High Performance Liquid Chromatography. *Journal of Chromatographia*, 50, 607-610.
- Katagi, T. (2004). Photodegradation of pesticides on plant and soil surfaces. *Journal of Environmental Contamination Toxicology*, 182, 1-195.
- Kathleen, C. (2000). Synthetic organo- and polymer-clays: preparation, characterization and materials application. *Applied Clay Science*, 17, 1-23.
- Kurkova, M., Praus, P. and Klika, Z. (2000). Using capillary isotachopheresis for the study of intercalation of quaternary salts into montmorillonite. *Journal of Chemistry Listy*, 94, 241-244.
- Lagaly, G., Ogawa, M. & Dekany, I. (2006). Clay mineral organic interactions. *Handbook of Development of Clay Science*, 7, 310-317.
- Lewis, D. & McConchie, D. (1994). Analytical Sedimentology. London; New York: Chapman and Hall 1, 144-145.
- Lugwisha, E. (2011). Identification of clay minerals of the Eastern Southern region of Lake Victoria by ethylene glycol and heat: x-ray diffraction and infrared spectroscopy studies. *Tanzanian Journal of Science*, 37, 168-178.
- Majedove, J. (2003). FTIR techniques in clay minerals studies, Vibrational Spectroscopy. *Journal of Elsevier*, 1, 1-10.

- Mann, R. S. & Kafman, P.E. (2012). Natural pesticide product: their development, delivery and use against insect ventors. *Journal of Mini-reviews in organic chemistry*, 9, 185-202.
- Masiwa, P. (2004). Evaluation of African diatomaceous earth (DEs) as potential maize protectant against the maize weevils (*Sitophilus zeamais*). BSc thesis.
- Mehlich, A. (1938). Use of triethanolamine acetate-barium hydroxide buffer for the determination of some base properties and lime requirements of soil. *Journal of Soil Science Society American Proceedings* 29, 374-378.
- Misra, L. & Dhara, S. (2011). Application of total reflection X-ray fluorescence spectrometry for trace elemental analysis of rain water. *Journal of Physics*, 76, 361-366.
- Mitic-Stojanovic, D., Bojic, D., Radovic, & M., Bojic, J. (2012). Equilibrium and kinetics of PbII, Cd II and Zn II sorption by *Lagenaria vulgaris* Shell. *Journal of Chemical Industry and Chemical Engineering Quarterly*, 18, 563-576.
- Monshi, A., Foroughi, R. M, Monshi, R. M. (2012). Modified Scherrer Equation to estimate more accurate nano-crystallite size using XRD. *World Journal of Nano Science and Engineering*, 2, 154-160.
- Moore, D. & Reynolds, R. (1989). X-ray diffraction and the identification and analysis of clay minerals, Oxford University Press, Oxford.
- Morris, S., Davies, P. & Groom, T. (2006). Effect of drying conditions on pyrethrins contents. *Journal of Indian Crop Production*, 23, 9-14.
- Mulungu, L., Lupenza, G., Reuben, S. & Misangu, R. (2007). Evaluation of botanical products a stored maize grain protectant against maize weevils, *Sitophilus zeamays* (L) on maize. *Journal of Entomology*, 4, 258-262.
- Muriithi, N., Karoki, K. & Gachanja, A. (2012). Chemical and mineral analyses of Mwea clays. *International Journal of Physical Science*, 44, 5865-5869.
- Musleh, M., Ahmad, A. & Eldurini, M. (2014). Characterization of Jordanian raw bentonite and surfactant-modified bentonite and their use in the removal of

- selected organic pollutants from aqueous solutions. *Journal of Applicable Chemistry*, 3: 823-833.
- Muzemu, S., Chitamba, J. & Goto, S. (2013). Screening of stored maize ( *Zea mays*L.) varieties grain for tolerance against maize weevil, *Sitophilus zeamais* (Motsch). *International Journal of Plant Research*, 3, 17-22.
- Muzemu, S., Chitamba, J. & Mutetwa, B. (2013). Evaluation of *Eucalyptus tereticornis*, *Tagetes minuta* and *Carica papaya* as stored maize grain protectants against *Sitophilus zeamais*(Motsch.) (Coleoptera, Curculionidae). *Journal of Agriculture, Forestry and Fisheries*, 2, 196-201.
- Namasivayam, C. & Sureshkuar, M. (2007). Removal of sulfate from water and wastewater by surfactant modified coir pith, an agricultural solid ‘waste’ by adsorption methodology. *Journal of Environmental and Management*, 17, 129-135.
- Navratilova, Z., Wojtowicz, P., Vaculikova, L. & Sugarkova, V. (2007). Sorption of alkylammonium cations on montmorillonite. *Journal of Acta Geodynamica Geomaterialia*, 4, 59-65.
- Nayak, S. & Singh, K. (2007). Instrumental characterization of clay by XRF, XRD and FTIR. *Journal of Bulletin of Material Science*, 30, 235-238.
- Nennemann, A., Mishaal, Y., Nir, S., Rubin, B., Polubesova, T., Bergaya, F., VanDamme, H. & Lagaly, G. (2001). Clay-based formulations of metolachlor with reduced leaching. *Journal of Applied Clay Science*, 18, 265-275.
- Neuwirthova, L., Matejka, V., Kutlakova, M. K. & Tomasek, V. (2012). X-ray fluorescence spectrometry analysis of clay/ZnO composites. *Journal of Nanoconductor*, 10, 23-25.
- Ngamo, T., Goundoum, A., Ngassoum, M., Mapongmetsem, L., Lognay, G., Malaisse, F. & Hance, T. (2015). Chronic toxicity of essential oils of three local aromatic plants towards *Sitophilus zeamais* Motsch. (Coleoptera, Curculionidae). *African Journal of Agricultural Research*, 2, 164-167.

- Njoka, E., Ombaka, O., Gicumbi, J., Kibaara, D. & Nderi, O. (2015). Characterization of clays from Tharaka-Nithi county in Kenya for industrial and agricultural applications. *African Journal of Environmental Science and Technology*, 9, 228-243.
- Okomoda, T., Solomon, G., Ataguba, A., Ayuba, O. & Asuwaju, F. (2013). Acute toxicity test in aquaculture, a review. *Banat's Journal of Biotechnology*, 4, 4738-4759.
- Oumabady, N., Rajendran, M. & Selvaraju, R. (2014). Mineralogical identification on polluted soils using XRD method. *Journal of Environmental Nanotechnology*, 3, 23-29
- Ouzaouit, N., Abdennouri, K., Mohamed El, M. (2013). Dried Prickly Pear Cactus (*Opuntia Ficus Indica*) cladodes as a low-cost and eco-friendly biosorbent for dyes removal from aqueous solutions. *Journal of the Taiwan Institute of Chemical Engineers*, 44, 52-60.
- Paiva, B., Morales, R. & Diaz, V. (2008). Organo clays, properties, preparation and applications. *Applied Clay Science*, 42, 8-24.
- Parimala, V. & Maheswari, U. (2013). Evaluation of selected insecticides as seed protectant against the maize weevil (*Sitophilus zeamais* M.). *International Journal of Applied Biology and Pharmaceutical Technology*, 2, 316-322.
- Patil, A. & Shrivastava, S. (2010). Removal of Cu (II) ions by *Leucaena Leucocephala* (Subabul) seed pods from aqueous solutions. *European Journal of Chemistry*, 7, 377-385.
- Pavlovic, D., Buntic, V., Siler-Marinkovic, S., Antonovic, G., Milutinovic, D., Radovanovic, R. & Dimitrijevic-Brankovic, I. (2014). Spent coffee grounds as adsorbents for pesticide paraquat removal from its aqueous solution. *International Conference on Civil, Biological and Environmental Engineering (CBEE-2014)* may 10, 27-28, Istanbul (turkey).

- Praus, P., Turicova, M., Studentova, S. & Ritz, M. (2006). Study of cetyltrimethylammonium and cetylpyridinium adsorption on montmorillonite. *Journal of Colloid and Interface Science*, 304, 29-36.
- Ravisankar, R., Senthilkumar, G., Kiruba, S., Chandrasekaran, A. & Prince, J. (2010). Mineral analysis of coast sediment samples of Tuna, Gujarat, India. *Indian Journal of Science and Technology*, 7, 1169-1174.
- Saikia, B. & Parthasarathy, G. (2014). Fourier transform infrared spectroscopic characterization of kaolinite from Assam Meghalaya, northeastern India. *Journal of Modern Physics* 1, 206-210.
- Sola, P., Mvumi, B., Ogendo, J. & Mponda, O. (2014). Botanical pesticide production, trade and regulatory mechanisms in sub-Saharan Africa: making a case for plant based pesticidal products. *Journal of Food Science* 10, 0343-0347.
- Thambavani, S. & Kavitha, B. (2014). Mineralogical characterization of river bed soil from Tamilnadu by FT-IR, XRD & SEM/EDAX. *International Journal of Advanced Research* 2, 656-659.
- Thavamani, S. & Rajikumar, R. (2013). Removal of Cr (VI), Cu(II), Pb(II) and Ni(II) from aqueous solution by adsorption on alumina. *Research Journal of Chemistry Science*, 3, 44-48.
- Ufele, A. N., Nnajidenma, U. P., Ebenebe, C. I., Mogbo, T. C., Aziagba, B.O. & Akunne, C. E. (2013). The effect of *Azadirachta indica* (Neem) leaf extract on longevity of snails (*Achatina achatina*). *International Research Journal of Biological Sciences*, 2, 61-63.
- Veli, S. & Alyuz, B. (2007). Adsorption of copper and zinc from aqueous solutions by using natural clay. *Journal of Hazardous Materials*, 149, 226-233.
- Viani, A., Gualtieri, F. & Artioli, G. (2002). The nature of disorder in montmorillonite by simulation of x-ray powder patterns. *Journal of American Mineralogist*, 87, 966-975.
- Wanyika, H. (2012). Development of nanostructured smart delivery systems for pesticides and fertilizers, PhD Thesis, J.K.U.A.T.

- Wanyika, H. (2014). Controlled release of agrochemicals intercalated into montmorillonite interlayer space. *The Scientific World Journal*, 10, 1-9.
- Wanyika, H., Kareru, P., Kenji, G., Keriko, J., Gachanja, A. & Mukiira, N. (2009). Contact toxicity of some fixed plant oils and stabilized natural pyrethrum extracts against adult maize weevils (*Sitophilus zeamais* Motschulsky). *Journal of African Pharmacy*, 3, 066-069.
- Wong, T., Wong, N. & Tanner, P. (1997). A fourier transform IR study of the phase transitions and molecular order in the hexadecyltrimethylammonium sulfate/water system. *Journal of Colloid and Interface*, 186, 325-331.
- Yankan, S., Kerkmann, R. & Yanik, T. (2015). Investigation effects environmental pollution on aquatic life. *Journal of Global Illuminators*, 1, 163-168.
- Yankachi, R. & Gadache, H. (2010). Grain protectant efficacy of certain plant extracts against rice weevils, *Sitophilus Oryzae* L. (Coleopteran, Curculionidae). *Journal of Biopesticides*, 3, 511-513.
- Yunfei, Xi., Ray, L. & Frost, Hongping He. (2007). Modification of the surfaces of Wyoming montmorillonite by the cationic surfactants alkyl trimethyl, dialkyl dimethyl and trialkyl methyl ammonium bromides. *Journal of Colloid and Interface Science*, 305, 150-158.
- Zhu, J., He, H., Zhu, L., Wen, X. & Deng, F. (2005). Characterization of organic phases in the interlayer of montmorillonite using FTIR and <sup>13</sup>C NMR. *Journal of Colloid Interface Science*, 286, 239-244.
- Zhu, L., Zhu, R., Xu, L. & Ruan, X. (2007). Influence of clay charge densities and surfactant loading amount on the microstructure of CTMA-montmorillonite hybrids. *Journal of Colloids Surfactant*, 304, 41-48.

## APPENDICES

**Appendix 1: Mean ( $\bar{x} \pm SD$ ) elemental composition (ppm) of different clay samples**

Element	A	B	C	D
K	168 ± 10	122 ± 22	116 ± 16	176 ± 20
Ca	322 ± 24	326 ± 24	633 ± 30	197 ± 30
Ti	20.0 ± 4	16.4 ± 4.2	18.9 ± 6.4	33.1 ± 6.8
V	30.2 ± 8.4	20.7 ± 6.2	31.3 ± 8.2	46.3 ± 6.6
Cr	25.5 ± 4.6	17.4 ± 4.2	22.8 ± 3.8	34.6 ± 3.6
Mn	149.3 ± 24	55.7 ± 6.8	79.4 ± 2.6	407 ± 22
Fe	3109 ± 144	2057 ± 158	2241 ± 126	3840 ± 28
Cu	0.213 ± 0.001	0.12 ± 0.00	0.12 ± 0.02	0.230 ± 0.4
Zn	6.85 ± 0.4	4.86 ± 0.6	5.73 ± 0.6	6.98 ± 0.8
As	0.1 ± 0.01	0.1 ± 0.02	0.1 ± 0.01	0.1 ± 0.02
Rb	6.55 ± 0.6	5.23 ± 0.4	4.80 ± 0.8	6.21 ± 0.4
Sr	2.72 ± 0.06	3.30 ± 0.08	5.94 ± 0.04	2.20 ± 0.02
Y	11.8 ± 0.4	10.1 ± 0.2	12.4 ± 0.4	12.5 ± 0.6
Pb	4.89 ± 0.2	3.06 ± 0.1	3.68 ± 0.2	7.92 ± 0.4

**Appendix 2: Crystallite clay size**

Peak	2 $\Theta$	$\Theta$	d (Å)	Miller Indices (hkl)	FWHM
(1)	7.94	3.94	9.6849	001	0.6543
(2)	16.09	8.045	4.8424	002	0.5420
(3)	27.61	13.805	3.2283	112	0.2800
(4)	28.95	14.475	3.1393	113	0.2800
Average crystallite size = $3.6894 \text{ \AA} = 36.894 \text{ nm}$					

**Appendix 3: The CEC of magnesium ions in clay samples**

Sample	Mg conc.	Dilution factor	Ppm	CEC(meq)
A	1.1236	500	561.8	4.6817 $\pm$ 0.04
B	0.1894	500	94.7	0.7892 $\pm$ 0.01
C	0.9848	500	492.4	4.1033 $\pm$ 0.08
D	1.288	500	644	5.3667 $\pm$ 0.2

**Appendix 4: The CEC of calcium ions in clay samples**

Sample	Ca Conc.	Dilution factor	ppm	CEC(meq)
A	0.0012	500	0.6	0.003 $\pm$ 0.0001
B	0.0001	500	0.055	0.0003 $\pm$ 0.00002
C	0.0014	500	0.6995	0.0035 $\pm$ 0.0003
D	0.0004	500	0.175	0.0009 $\pm$ 0.00002

**Appendix 5: The CEC of sodium ions in clay samples**

Sample	Na Conc.	Dilution factor	ppm	CEC(meq)
A	37.3625	500	18681.25	81.22 ± 6
B	30.195	500	15097.5	65.64 ± 8
C	37.9725	500	18986.25	82.55 ± 10
D	38.2775	500	19138.75	83.212 ± 8

**Appendix 6: The CEC of potassium ions in clay samples**

Sample	K. Conc.	Dilution factor	ppm	CEC(meq)
A	2.5365	500	1268.3	3.252 ± 0.1
B	1.0146	500	507.3	1.301 ± 0.03
C	1.7756	500	887.7	2.2764 ± 0.4
D	1.2683	500	634.13	1.6260 ± 0.2

**Appendix 7: Sorption capacity of PFE at different pH in various clay samples**

Sorption capacity			
pH	Un-modified clay	TMPA clay	HDTMA clay
3	21.5 ± 4.2	26.1 ± 3.1	27.5 ± 1.6
3.6	22.5 ± 6.4	25.4 ± 4.2	29.4 ± 2.8
4	20.3 ± 4.8	24 ± 3.8	32.2 ± 4.7
4.6	19.4 ± 1.4	23 ± 4.6	37.2 ± 1.3
5	13 ± 3.8	21.4 ± 5.5	40.4 ± 2.6
6	1.6 ± 4.5	3.5 ± 0.8	5 ± 0.5
7	1 ± 1.1	3 ± 0.3	5 ± 0.6

**Appendix 8: Sorption capacity of PFE at different adsorbate dose in various clay samples**

Sorption capacity			
Adsorbate Dose(g)	Un-Modified clay	HDTMA Clay	TMPA clay
0.1	27.8 ± 3.5	28.3 ± 2.1	25.3 ± 3.2
0.2	35.4 ± 2.2	58.1 ± 4.6	52.1 ± 3.6
0.25	39 ± 6.6	61.6 ± 1.3	52.6 ± 4.7
0.5	45.4 ± 3.3	83.12 ± 5.4	66.8 ± 3.8
1	60.5 ± 4.5	97.24 ± 4.3	75.5 ± 5.4
1.5	60.5 ± 5.6	97.2 ± 6.5	75.5 ± 3.3

**Appendix 9: Langmuir concentration at equilibrium versus sorption capacity of various clay materials**

Ce/ Qe	Un-Modified (Ce)	Ce/ Qe	TMPA (Ce)	Ce/ Qe	HDTMA (Ce)
0.052±0.07	2.6255	0.059 ± 0.1	2.6162	0.051 ± 0.1	2.5107
0.037±0.05	2.2101	0.018 ± 0.06	1.6753	0.017±0.06	1.5909
0.028±0.08	1.9004	0.014 ± 0.11	1.6576	0.014±0.13	1.465
0.027±0.05	1.9126	0.0099±0.05	1.1615	0.013±0.07	1.3435
0.013 ± 0.1	1.5191	0.0064±0.16	0.3499	0.001 ± 0.1	0.0965
0.013 ± 0.1	1.5191	0.0064±0.08	0.3499	0.001±0.08	0.0965

**Appendix 10: Freundlich concentration at equilibrium versus sorption capacity in  
different clay materials**

Log Qe	Un-Modified (Ce)	Log Qe	TMPA (Ce)	Log Qe	HDTMA (Ce)
1.6878± 0.1	2.5255	1.6953±0.15	2.6162	1.6943±0.1	2.8107
1.7924±0.15	2.2601	1.9602±0.16	1.7653	1.9798±0.2	1.4509
1.7342±0.062	2.1349	1.9644±0.05	1.6576	2.0075±0.15	1.335
1.9997± 0.09	1.9126	2.1079± 0.2	1.1615	2.0327± 0.1	1.2035
2.025± 0.14	1.3791	2.1823±0.08	0.8499	2.2309±0.14	0.19
2.025± 0.08	1.3791	2.222± 0.1	0.7499	2.2509± 0.1	0.1065

**Appendix 11: Pseudo first order values for sorption of PFE in various clay materials**

Un-Modified Clay					
Log (Qe - Qt)					
Time	3.5µg/ mL	2.5µg/ mL	2.0 µg/ mL	1.5 µg/mL	1.0 µg/ mL
0	1.91	1.9693	1.2149	1.7391	1.6243
10	1.7278	1.6267	1.7145	1.8686	1.7575
30	1.5878	1.6901	1.4717	1.643	1.4636
60	1.7472	1.6073	1.5499	1.5545	0.9745
90	1.3014	1.2035	1.3338	1.3106	0.4579
120	0	0	0	0	0
TMPA-Clay					
Log (Qe-Qt)					
Time	3.5µg/ mL	2.5µg/ mL	2.0 µg/ mL	1.5 µg/ mL	1.0 µg/ mL
0	2.1022	2.1504	1.7716	1.9251	1.8516
10	1.8461	1.9147	1.9294	1.9193	1.8608
30	1.7072	1.7568	1.6488	1.6796	1.7248
60	1.5236	1.6786	1.2885	1.2521	1.2598
90	1.1926	0.8932	0.6609	0.9557	0.9036
120	0	0	0	0	0
HDTMA-Clay					
Log (Qe-Qt)					
Time	3.5µg/ mL	2.5µg/ mL	2.0 µg/ mL	1.5 µg/ mL	1.0 µg/ mL
0	2.3309	2.1771	2.0924	2.1389	1.9685
10	2.0917	2.1491	2.0068	1.9572	1.1922
30	1.9945	1.9924	1.789	1.953	1.7433
60	1.966	1.681	1.5259	1.5202	1.4888
90	1.1679	1.2167	1.2014	1.2343	1.5233
120	0	0	0	0	0

**Appendix 12: Pseudo second order values for sorption of PFE in various clay materials**

Un- Modified Clay					
(Qt)					
Time	3.5 µg/ml	2.5 µg/ml	2.0 µg/ml	1.5 µg/ml	1.0 µg/ml
0	0	0	0	0	0
10	0.2582	0.1836	0.4623	0.0971	0.2667
30	0.5172	0.479	0.5987	1.0956	1.5789
60	0.7692	0.9835	1.3138	1.4793	1.8366
90	0.9639	1.1183	1.3238	1.7046	2.2942
120	1.1332	1.288	1.4937	2.5382	2.8504
150	1.4151	1.6099	2.3671	2.8727	3.5629
TMPA Modified Clay					
(Qt)					
Time	3.5 µg/ml	2.5 µg/ml	2.0 µg/ml	1.5 µg/ml	1.0 µg/ml
0	0	0	0	0	0
10	0.2263	0.1818	0.2623	0.0695	0.1063
30	0.3211	0.4437	0.6106	0.4255	0.4381
60	0.6053	0.73	0.8082	0.9051	1.1351
90	0.7697	0.8614	1.0102	1.1979	1.4277
120	0.9056	1.0686	1.2811	1.4259	1.989
150	1.132	1.3357	1.6014	1.7823	2.4112
HDTMA Modified Clay					
(Qt)					
Time	3.5 µg/ml	2.5 µg/ml	2.0 µg/ml	1.5 µg/ml	1.0 µg/ml
0	0	0	0	0	0
10	0.0621	0.0904	0.0919	0.0926	0.1082
30	0.167	0.2257	0.2924	0.3659	0.347
60	0.3445	0.3986	0.5856	0.5843	0.6748
90	0.5289	0.5922	0.8348	0.8732	1.0358
120	0.7051	0.7981	1.107	1.1946	1.3502
150	0.8814	0.9976	1.3925	1.4682	1.7027

**Appendix 13: Percentage PFE degraded both in different clay materials and in un-protected (control) PFE**

Sample	Radiations	% PFEdegraded in clay materials	Sample	Radiations	% Un-protected PFE degraded (Control)
Un-Modified Clay	254 nm	8.85 ± 0.5	Un-Modified Clay	254 nm	67.28 ± 5.1
	366 nm	54.33 ± 5.1		366 nm	76.33 ± 7.3
	Natural sunlight	44.2 ± 3.2		Natural sunlight	88.33 ± 9.2
TMPA Clay	254 nm	5.29±0.9	TMPA Clay	254 nm	61.81±6.1
	366 nm	41.87±7.1		366 nm	67.48±10.1
	Natural sunlight	52.41±4.3		Natural sunlight	86.93 ± 7.3
HDTMA Clay	254 nm	5.51 ± 1.2	HDTMA Clay	254 nm	68.17± 8.4
	366 nm	21.35 ± 6.1		366 nm	75.88 ±7.2
	Natural sunlight	36.6 ± 2.3		Natural sunlight	88.87± 12.1

**Appendix 14: Effect of different treatments on *Sitophilus zeamais* mortality rate**

% Mortality rate						
Treatments	Dose	24 hours	48 hours	72 hours	96 hours	120 hours
PFE- HDTMA clay	0.1	15 ± 1	36.5 ± 1.2	65 ± 1.53	95 ± 1.0	100 ± 1.73
	0.5	26.5±0.58	58 ± 1.53	99.5±1.53	99.5±1.53	99.5±1.53
PFE- TMPA clay	0.1	16.5±0.58	28 ± 0.58	49.5±1.53	63 ± 0.58	79 ± 0.58
	0.5	21.5±0.58	41.5±1.0	76.5 ± 1.0	81.5 ± 1.0	92.5 ± 1.0
PFE-clay	0.1	1.5 ± 0.58	5 ± 0.58	15 ± 1	26.5±0.58	40 ± 0.58
	0.5	6.5 ± 0.58	16.5 ± 1	36.5 ± 1	59.5±1.53	81 ± 0.58
HDTMA- clay	0.1	3.5 ±0.58	5 ± 0.58	6.5 ± 0.58	8 ± 0.58	11.5 ± 1
	0.5	3.5 ± 0.58	7 ± 1.2	17 ± 1.2	25 ± 0.58	30 ± 0.58
TMPA-clay	0.1	0 ± 0.58	3.5 ± 0.58	7 ± 0.58	10.5±0.58	11.5 ± 1
	0.5	1.5 ± 0.58	6.5 ± 1	13 ± 1.2	18 ± 0.58	23 ± 1
Clay	0.1	1.5 ± 0.58	3± 0.58	6.5 ± 0.58	10±0.58	11.5±0.58
	0.5	1.5 ± 0.58	8 ± 1.2	18±1	23±1	29.5±0.58
Un- degraded PFE	0.1	62 ± 2	89 ± 1.3	100 ± 4.0	100 ± 4.0	100 ± 4.0
	0.5	74 ± 1.5	100 ± 2.5	100 ± 2.5	100 ± 2.5	100 ± 2.5
Degraded PFE	0.1	0 ± 0	1.5 ± 0.58	3 ± 0.58	6.5 ± 0.58	6.5 ± 0.0
	0.5	1.5 ± 0.58	16.5 ± 1.2	18 ± 1	23 ± 1	29.5±0.58

**Appendix 15: FT-IR Spectra of (a) HDTMA and (b) TMPA organic cations**

